AFATL-TR-88-143

A Comprehensive Review of Modeling of Impact Damage in Ceramics

A M Rajendran
W H Cook

UNIVERSITY OF DAYTON RESEARCH INSTITUTE
DAYTON, OHIO 45469

DECEMBER 1988

FINAL REPORT FOR PERIOD MARCH - OCTOBER 1988

AIR FORCE ARMAMENT LABORATORY
Air Force Systems Command ▮ United States Air Force ▮ Eglin Air Force Base, Florida

NOTICE

When Government drawings, specifications, or other data are used for any purpose other than in connection with a definitely related Government procurement operation, the United States Government thereby incurs no responsibility nor any obligation whatsoever; and the fact that the Government may have formulated, furnished, or in any way supplied the said drawings, specifications, or other data, is not to be regarded by implication or otherwise as in any manner licensing the holder or any other person or corporation, or conveying any rights or permission to manufacture, use, or sell any patented invention that may in any way be related thereto.

This report has been reviewed by the Public Affairs Office (PA) and is releasable to the National Technical Information Service (NTIS). At NTIS, it will be available to the general public, including foreign nations.

This technical report has been reviewed and is approved for publication.

FOR THE COMMANDER

HOWARD J. BUSH, Colonel, USAF
Chief, Munitions Division

If your address has changed, if you wish to be removed from our mailing list, or if the addressee is no longer employed by your organization, please notify AFATL/MNW , Eglin AFB FL 32542-5434.

Copies of this report should not be returned unless return is required by security considerations, contractual obligations, or notice on a specific document.

Unclassified
SECURITY CLASSIFICATION OF THIS PAGE

REPORT DOCUMENTATION PAGE

Form Approved OMB No. 0704-0188

1a. REPORT SECURITY CLASSIFICATION Unclassified	1b. RESTRICTIVE MARKINGS
2a. SECURITY CLASSIFICATION AUTHORITY	3. DISTRIBUTION/AVAILABILITY OF REPORT Approved for public release; distribution is unlimited.
2b. DECLASSIFICATION/DOWNGRADING SCHEDULE	
4. PERFORMING ORGANIZATION REPORT NUMBER(S)	5. MONITORING ORGANIZATION REPORT NUMBER(S) AFATL-TR-88-143
6a. NAME OF PERFORMING ORGANIZATION Univ. of Dayton Research Inst. Air Force Armament Laboratory 6b. OFFICE SYMBOL (If applicable) MNW	7a. NAME OF MONITORING ORGANIZATION Warheads Branch Munitions Division
6c. ADDRESS (City, State, and ZIP Code) Dayton, OH 45469 Eglin Air Force Base, FL 32542	7b. ADDRESS (City, State, and ZIP Code) Air Force Armament Laboratory Eglin Air Force Base, FL 32542
8a. NAME OF FUNDING/SPONSORING ORGANIZATION Munitions Division 8b. OFFICE SYMBOL (If applicable) AFATL/MNW	9. PROCUREMENT INSTRUMENT IDENTIFICATION NUMBER F33615-86-C-5064
8c. ADDRESS (City, State, and ZIP Code) Air Force Armament Laboratory Eglin Air Force Base, FL 32542-5434	10. SOURCE OF FUNDING NUMBERS

PROGRAM ELEMENT NO.	PROJECT NO.	TASK NO.	WORK UNIT ACCESSION NO.
62602F 62601F	2502 2302	07 E2	01 11

11. TITLE (Include Security Classification)

A Comprehensive Review of Modeling of Impact Damage in Ceramics

12. PERSONAL AUTHOR(S)

A.M. Rajendran, W.H. Cook

13a. TYPE OF REPORT	13b. TIME COVERED	14. DATE OF REPORT (Year, Month, Day)	15. PAGE COUNT
Final	FROM Mar 88 TO Oct 88	December 1988	100

16. SUPPLEMENTARY NOTATION

This report was a joint effort between the University of Dayton Research and the Air Force Armament Laboratory. Therefore, the report is in contract format.

17. COSATI CODES			18. SUBJECT TERMS (Continue on reverse if necessary and identify by block number)
FIELD	GROUP	SUB-GROUP	Ceramic, Fracture, Impact, Failure Models
11	02		
19	10		

19. ABSTRACT (Continue on reverse if necessary and identify by block number)

This report reviews high strain rate experimental and analytical methods available for characterizing ceramic material behavior. Also, a discussion on the ceramic failure mechanisms upon impact loading conditions is provided. Theoretical basis for constitutive and failure modeling of ceramic type brittle material is discussed. Models that are reported in open literature are reviewed and categorized based on their theoretical approaches. The salient features of a few recently reported constitutive/damage theories, which combine either the micromechanics or the continuum damage mechanics for the stress-strain relationship with fracture mechanics for damage accumulation description, are described and tabulated. Recent attempts to employ such models in the computer calculation of armor penetration problems are briefly discussed.

20. DISTRIBUTION/AVAILABILITY OF ABSTRACT	21. ABSTRACT SECURITY CLASSIFICATION
☐ UNCLASSIFIED/UNLIMITED ☒ SAME AS RPT. ☐ DTIC USERS	Unclassified

22a. NAME OF RESPONSIBLE INDIVIDUAL	22b. TELEPHONE (Include Area Code)	22c. OFFICE SYMBOL
William H. Cook	(904)882-2145	AFATL/MNW

DD Form 1473, JUN 86 *Previous editions are obsolete.* SECURITY CLASSIFICATION OF THIS PAGE

Unclassified

PREFACE

This report describes a joint contractual and in-house effort conducted by personnel of the University of Dayton Research Institute and the Warheads Branch, Munitions Division, Air Force Armament Laboratory, Eglin Air Force Base, Florida 32542-5434, under projects 25020701 (Numerical Hydrodynamics) and 2302E211 (Ceramic Fracture).

The work reported herein was performed during the period 1 March 1988 to 30 October 1988. Partial support and funding for the Armament Laboratory portion of this effort were supplied by the Air Force Office of Scientific Research (AFOSR/NA). The AFATL program manager was Mr William H. Cook. Work performed at the University of Dayton Research Institute was under the direction of Dr Theodore Nicholas of the Air Force Wright Aeronautical Laboratories, Wright-Patterson AFB OH.

The authors wish to thank Mr Mark Dietenberger, Mr Tarabay Antoun, and Dr Reji John for their technical assistance in assembling this report. Also, the support and encouragement of Dr Joseph P. Gallagher (UDRI) and Mr Ron Boulet (AFATL/MNW) is gratefully acknowledged.

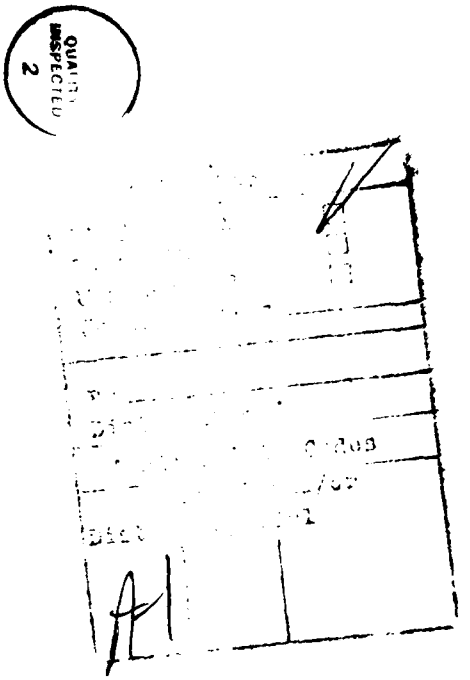

TABLE OF CONTENTS

TABLE OF CONTENTS (concluded)

LIST OF ILLUSTRATIONS

LIST OF ILLUSTRATIONS (continued)

LIST OF ILLUSTRATIONS (concluded)

LIST OF TABLES

SECTION 1
INTRODUCTION

Ceramic materials are increasingly being used as armor elements, engine turbine blades, and other structural elements because of their enhanced dynamic compressive strength and high temperature properties. Understanding of ceramic behavior under impact loading conditions is essential in the design of improved impact resistant materials for dynamic structural and armor applications. For instance, the study of damage due to the impact of a foreign object on ceramic turbine blades requires a critical evaluation of impact properties of ceramics.

This report reviews the status of both experimental and analytical studies on impact behavior of ceramic materials. An extensive literature search was conducted for this purpose. Journals, technical reports, and books that are available in the open literature were searched for suitable articles addressing the impact experiments and modeling of ceramic material behavior. Fracture mechanics based studies on a single crack geometry were not considered in the review. However, use of fracture mechanics concepts to describe micromechanical damage is reviewed and presented. In Section 2, background information is discussed regarding properties and applications of ceramic materials. Various impact experimental configurations and sample data from these configurations are presented in Section 3. Section 3 also includes a literature review of constitutive and failure models that describe the impact behavior of ceramic materials. Several candidate brittle models are compared and discussed in detail. Moreover, this section addresses the computational aspects of ceramic material characterization. Recent work on the simulation of metallic rod penetration into ceramic targets is also discussed. A brief summary of the review and future recommendations are presented in Section 4.

SECTION 2
BACKGROUND

Experimental studies on impact properties of various ceramics were initiated about 20 years ago (for example, Ahrens et al. [Reference 1], Gust and Royce [Reference 2], Gust et al. [Reference 3], Munson and Lawrence [Reference 4]). In these and in further [References 5-7] studies, the ceramics were characterized based on parameters such as density, elastic moduli, sound wave speed, porosity, and strength. For example, Gust et al. [3] evaluated the Hugoniot Elastic Limit (HEL) and determined the Hugoniot (in stress-volume space) for different ceramic materials. They attempted to correlate all data by plotting the dynamic compressive yield strengths of these materials against their respective shear moduli as shown in Figure 1. A linear relationship, $Y_o = 0.056$, can be used as a crude approximation for the data set studied. No physical basis has been proposed.

During the later part of the seventies, experimental impact studies on ceramics slowed down significantly until recently. There has been a renewed interest in recent years, focusing on the evaluation of impact behavior primarily through sophisticated plate impact experiments as well as constitutive and failure modeling of the results of these experiments. Increasing emphasis on modeling is due mainly to the expanded use of advanced finite element/finite difference codes in engineering design applications. To obtain realistic and dependable results from code calculations, an accurate description of material behavior is necessary. For this purpose, suitable models for the deformation and failure mechanisms in brittle ceramics are necessary. Development of advanced models for the accurate descriptions of ceramic behavior under impact loading conditions is an important next step in the area of ceramic material characterization.

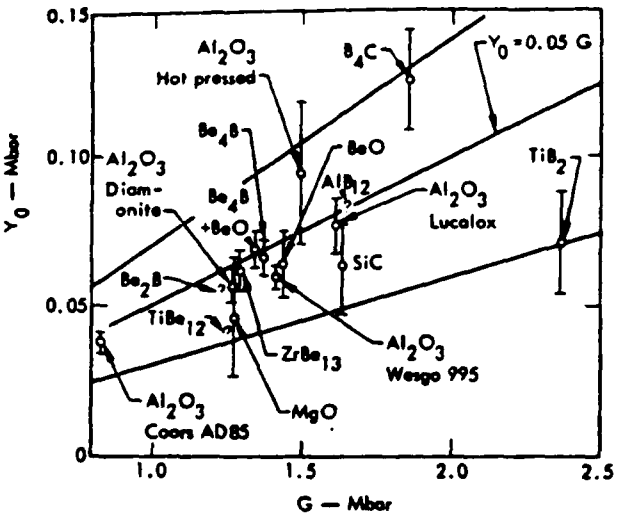

Figure 1. Dynamic compressive yield strength for 16 brittle high-strength materials plotted against their respective shear moduli. [3]

Only a limited number of ceramic materials have been evaluated for impact behavior, and even fewer have been characterized in terms of their dynamic material properties. Among the most predominant materials considered are Al_2O_3 alumina (commercial designations include AD-85, AD-95, AD-99, AL-300, and Lucalox), TiB_2, and BeO. A summary of some mechanical properties of these and other ceramic materials is given in Table 1. This table also provides a summary of some published dynamic material property data available in the literature and the sources of these data. Most of the data are discussed in the Literature Review Section that follows.

TABLE 1

Mechanical Properties of Some Ceramics

Material	Initial Density (g/cm^3)	Longitudinal Velocity (mm/μs)	Young's Modulus (Mbar)	Hugoniot Elastic Limit (kbar)	Reference
Sapphire	3.986	11.64	5.40	165±5	9
Sapphire-58° to C-axis	3.98	10.9	4.73	---	5
Sapphire-C-axis	3.985	11.34±0.1	5.13	---	10
Al_2O_3-95%-Lucalox	3.75	---	---	50	6
Al_2O_3-85%-Lucalox	3.40	---	---	45	6
Al_2O_3-Polycrystalline	3.969	10.9	4.72	91	4
Al_2O_3-Polycrystalline	3.98	10.94	4.76	112±13	1
Al_2O_3-Hot Pressed	3.92	10.59	4.40	126±34	2
Al_2O_3-Al-995	3.81	10.34	4.07	83±5	1
Al_2O_3-AD-85	3.42	8.84	2.67	61±5	2
Quartz-X-cut	2.65	5.70	0.86	42.5±7.5	11
Quartz-X-cut	2.65	6.36	1.07	72.5±7.5	11
Fused Quartz	2.2	5.97	0.78	98	11
Glass	2.48	5.85	0.85	73	7
B_4C-Polycrystalline	2.50	13.78	4.75	149.5±12.5	2
BeO-Polycrstalline	2.84	11.54	3.78	82.5±8.5	2
MgO-Single Crystalline	---	---	---	40	6
MgO-Single Crystalline (100)	3.57	9.34	3.11	63±26	13
MgO-Single Crystalline (100)	---	9.34	---	23±3	14
WC-Polycrystalline	---	---	---	40	6
SiC	3.09	11.40	3.78	86±30	3
TiB_2	4.51	11.21	5.41	80±30	3
Be_4B	1.98	12.42	2.99	74±10	3
Be_4B + 8% BeO	1.97	12.32	2.88	77±10	3
AlB_2	2.54	11.85	3.52	87±4	3
TiB_2	2.28	11.55	2.89	53	3
Be_2B	1.99	12.03	2.78	65	3
$Zr_{Be_{13}}$	2.73	10.38	2.85	71±12	3

SECTION 3
LITERATURE REVIEW

An extensive literature search was conducted at both the University of Dayton and Eglin Air Force Base for this report. It involved a thorough computer search of the pertinent DIALOG commercial data base for scientific periodicals, local libraries (including technical reports), and the Defense Technical Information Center. The literature search was conducted based on the following key words: ceramic impact, high strain rate, ceramic fracture, brittle fracture theory, microcracks, constitutive, stress-strain, dynamic failure, dynamic fracture, failure model, fracture model, etc. The search emphasized high strain rate or impact experimental investigations, impact failure processes in brittle materials, and analytical constitutive and failure modeling under both quasi-static and dynamic loading conditions. No attempt was made to document the quasi-static test techniques used to characterize ceramic type brittle materials.

3.1 EXPERIMENTS

To obtain realistic and dependable results from advanced large scale computer codes, the material behavior under impact loading conditions must be accurately described. This can be accomplished by using constitutive and failure models that can simulate the response of the material to dynamic loading conditions. In the case of ceramics, analytical models are still in the developmental stages and accurate predictions of the high strain rate response of the material, in the main, do not exist. In the process of developing better models, experimental investigations are of paramount importance. A reliable model that is capable of predicting the overall material response can be developed only through a better understanding of the underlying

mechanisms leading to the observed mechanical responses. With that in mind, the various high strain rate testing techniques are reviewed in the subsequent paragraphs. These techniques cover a wide range of stress and strain states. While the normal plate impact test leads to a uniaxial strain state in which all three stress components are non-zero, the split Hopkinson bar (SHB) test as well as the long rod impact test exert a uniaxial stress state in which all three strain components are non-zero. The review of experimental techniques also include the oblique plate impact test in which combined pressure and shear loading is applied. Double flyer plate test, plate impact recovery, and penetration experiments are also included in the review.

A summary of results obtained from the various experimental configurations are presented with the exception of the oblique plate impact test from which no ceramic data has been obtained. This test is included in this review for completeness and because it promises to be an invaluable tool in evaluating the pressure-shear behavior of pressure sensitive materials such as ceramics.

3.1.1 Normal Plate Impact

The most frequently reported experimental technique to characterize ceramics under impact is based on the flyer plate impact test configuration shown in Figure 2. In this configuration, a flyer plate is impacted against a target of the same or different material at high velocity. It is a standard laboratory test to determine the Hugoniot elastic limit (HEL) of a target material. The steady state value of the HEL is related to the compressive yield strength, Y_o, by:

$$Y_o = \frac{\sigma_{HEL}}{\{(K/2G) + (2/3)\}} \qquad (1)$$

where K and G are bulk and shear moduli, respectively.

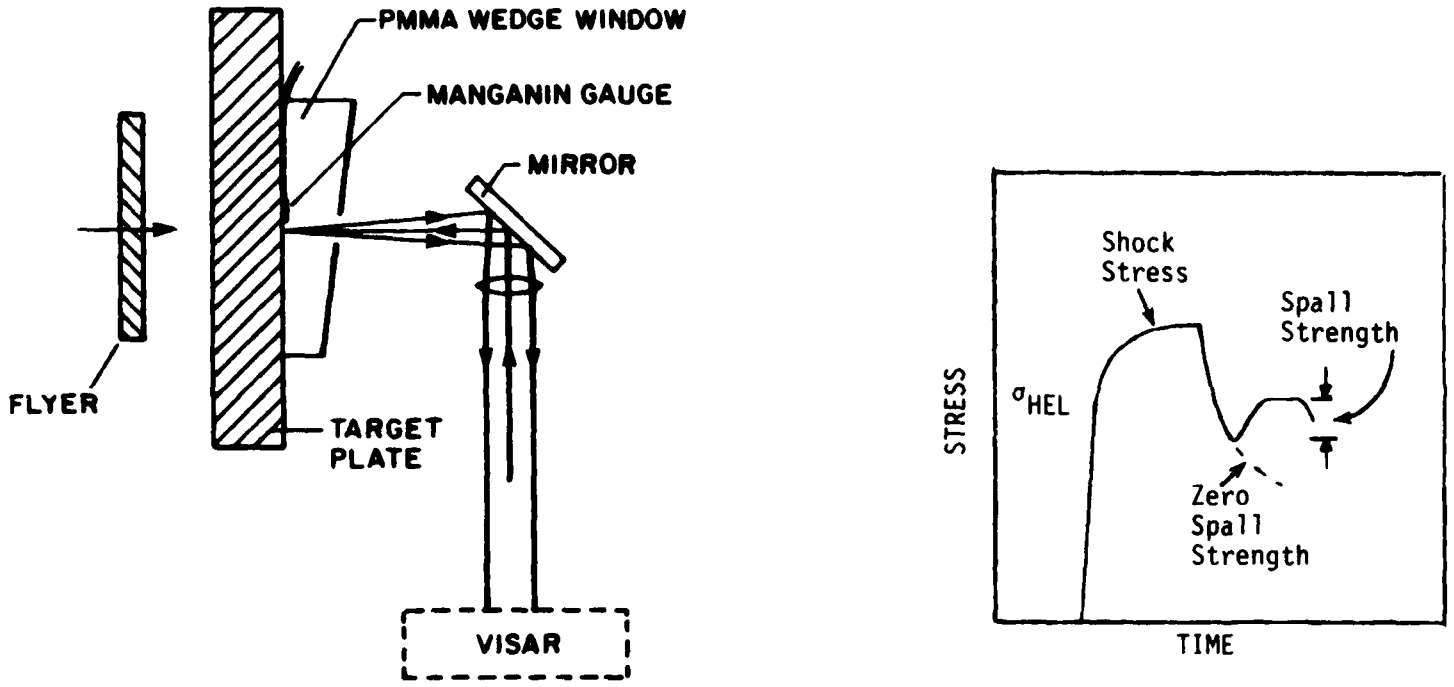

Figure 2. Schematic representation of the flyer plate impact test.

In ceramic materials, the HEL is considered as the maximum stress up to which the brittle ceramic material deforms in an elastic manner. Beyond that point, damage and/or apparent inelastic deformation occurs. Inelastic strains are primarily attributed to the nucleation of microcracks and their growth under compression. Munson and Lawrence [Reference 4] presented the behavior of polycrystalline Al_2O_3 based on plate impact test results. In their study, the dynamic stress-wave response was deduced from the particle velocity profiles obtained using VISAR (a velocity laser interferometer) measurements. These profiles showed an initial elastic wave followed by the onset of a second "plastic" wave which carried the material to the peak particle velocity as shown in Figure 3. The profiles exhibited significant rounding or dispersion beyond the onset point. This dispersive nature of the so called "plastic wave" indicated a strain rate dependent inelastic deformation process in Al_2O_3. The paper by Munson and Lawrence [Reference 4] seems to be the most cited earlier work on the impact behavior of a ceramic material. One of the most important observations in their study is the loss of strength in tension. The spall strength (or tensile strength) in Al_2O_3 was negligible (less than 0.05 GPa) when the impact velocity was above the HEL. The values did not appear to depend upon the amount of compressive deformation prior to tension.

The dynamic response of AD-85 alumina was studied by Rosenberg et al. [Reference 8] using in-material manganin gages. An AD-85 flyer, 6.2 mm thick plate was impacted on an AD-85 12.4 mm thick target. The calculated yield strength, Y_o, was 43 kbars (note that 1 kbar = 14504 psi or 100 MPa), corresponding to the HEL value of 60 kbars. This compressive strength is more than twice the static compressive strength. For Lucalox, Munson and Lawrence [Reference 4] reported that the ratio of dynamic to static strength was about 3. The drastic increase in compressive

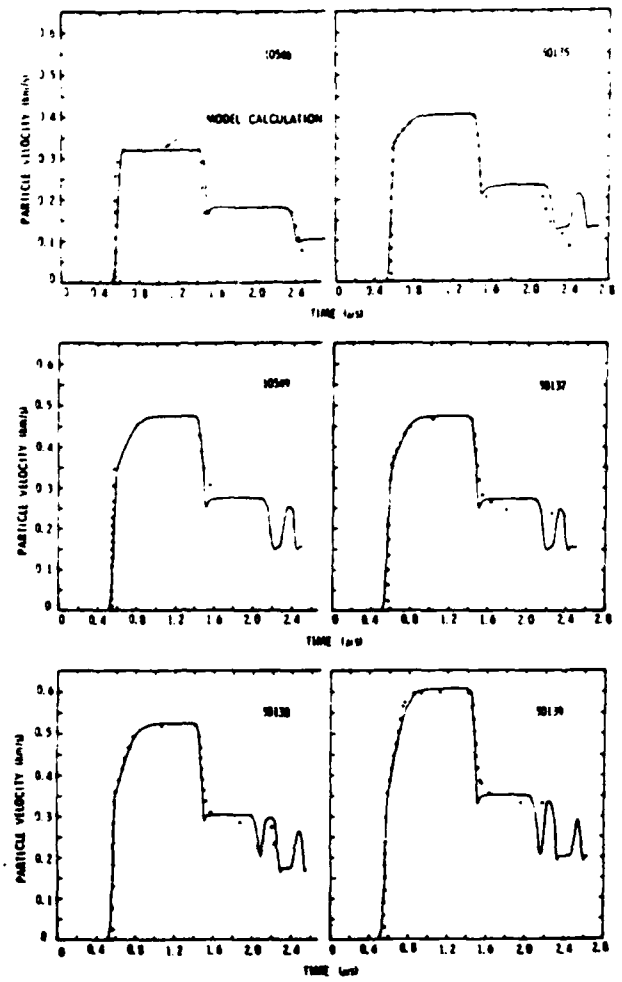

Figure 3. Particle-velocity profiles measured (dots) during the gun experiments, together with model calculations (lines). [4]

strength under plate impact loading has been reported for several ceramic materials [References 1,2]. It is also typical of ceramic materials to possess very low spall strength compared to their compressive strength.

During the seventies, plate impact tests on various brittle materials were reported. Sapphire was one of the most often cited generic materials used in several shock related studies [References 9,10]. It was found that the shear strength $(\sigma_x - \sigma_y)/2$ of sapphire is significantly reduced when the shock stress is at or above the HEL, as shown in Figure 4. It can be seen that beyond the HEL (A), instead of following the dotted line (as usually observed in metals), the Hugoniot curve jumps to point B and follows the curve BC which indicates loss of shear strength. This sudden loss of shear strength was also observed in several single crystals, such as quartz [References 11,12] and MgO [References 13,14,15]. Polycrystalline ceramics, however, in most cases do not lose their shear strength [16]. Rosenberg et al. [Reference 16] recently reported that the shear strength of AD-85 was around 50-55 Kbars, even up to a shock stress of 150 Kbars as can be seen from Figure 5. Their measurements involved the use of an embedded transverse gage as well as a longitudinal gage. The shear strength remained high under confining pressure until the release waves started to reduce the confining pressure. The comminuted material finally lost its apparent shear strength upon the removal of confining pressures. Several other investigators [References 2,17] also reported the reduction of shear strength during the release process in polycrystalline alumina.

Most of the brittle ceramic materials showed very low spall strength below, at, and above the HEL. Sodalime glass materials exhibited very high tensile strength (near the theoretical tensile strength limit) below the HEL [Reference 18]; however, the tensile strength rapidly decreased to zero when

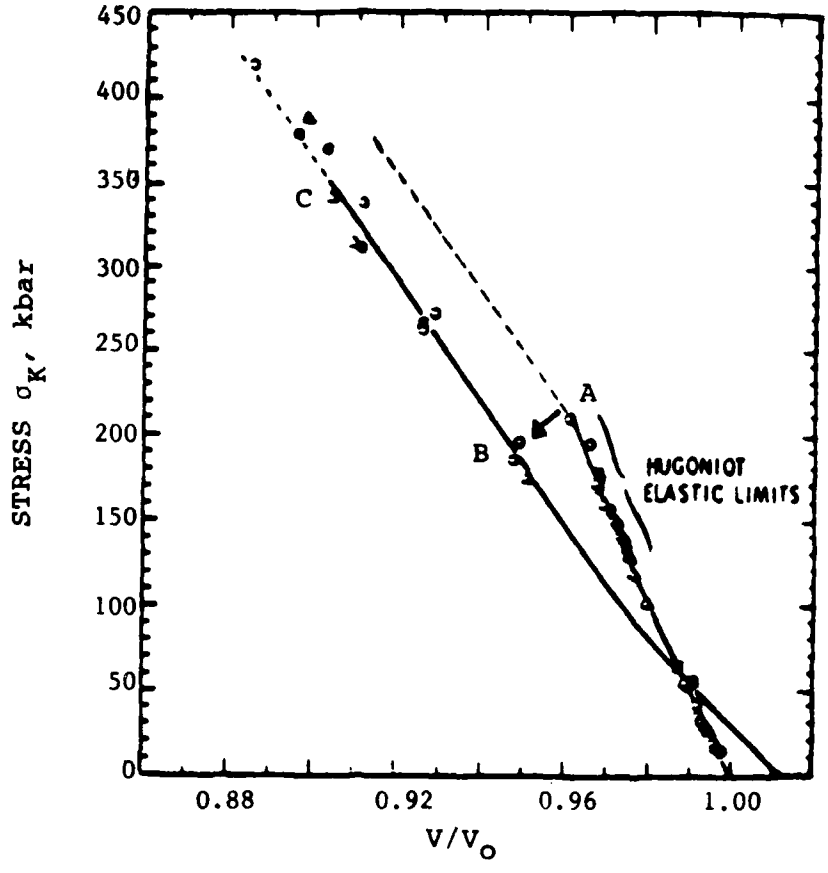

Figure 4. Stress-volume relations for sapphire under shock wave compression.

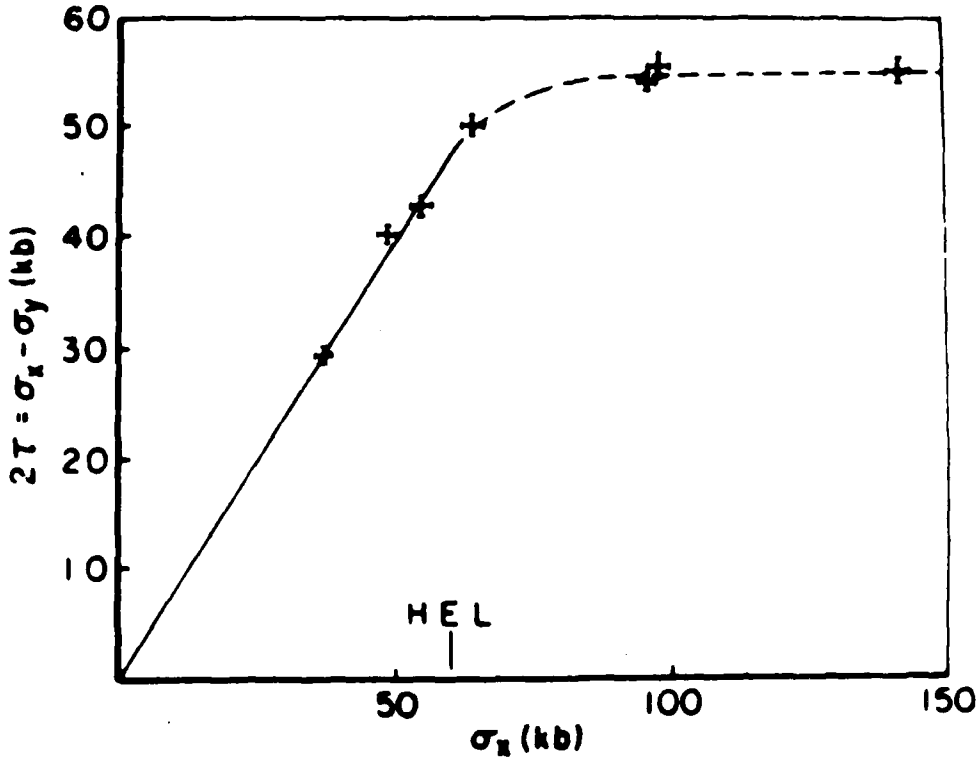

Figure 5. Variation of the shear strength of AD-85 with shock amplitude. [16]

sodalime glass was shocked to stresses slightly above the HEL. At the HEL, the tensile strength was zero as shown in Figure 6.

3.1.1.1 Precursor Decay

The precursor decay phenomenon which is usually observed in metals has also been frequently reported in ceramic materials [References 11,14,19,20]. Precursor decay is defined as the decay of the longitudinal stress amplitude (HEL) of the elastic wave (precursor) from a peak value at the plane of impact to a steady state value at some distance from the impact plane. Yaziv et al. [Reference 20] reported a strong precursor decay in commercial AD-85 alumina as shown in Figure 7. The HEL did not reach its steady state value even up to a distance of 40 mm through the target plate. Recently, Cagnoux and Longly [Reference 21] presented conflicting results based on the VISAR measurement for a commercial alumina (95% Al_2O_3) and concluded that this alumina did not exhibit any precursor decay as shown in Figure 8. In their study, plate impact experiments were performed to evaluate the rate dependence of the compressive strength of alumina at high strain rates. A glass ceramic material was used to generate a ramp wave into the target material. Results of the experiment showed no influence of strain rate on the HEL.

3.1.2 Advanced Flyer Plate Experimental Techniques

Two important aspects of the dynamic response of ceramics are the response under a combined pressure-shear loading and the damage response evolution. These responses cannot be studied using the normal plate impact test simply because a planar impact with the target face normal to the impact direction does not cause a shear wave to propagate into the target. Furthermore, the single impact, even if it causes spall, does not recompact the spall plane thus allowing for the determination of

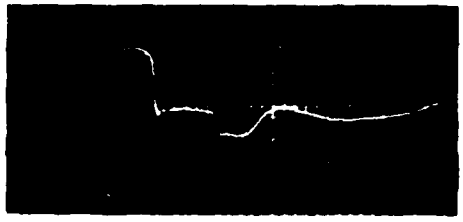

(a)

(b)

Figure 6. Gage records from (a) Exp. No. 889 (above the HEL) and (b) Exp. No. 892 (below the HEL). Time base is 1μs per division. [18]

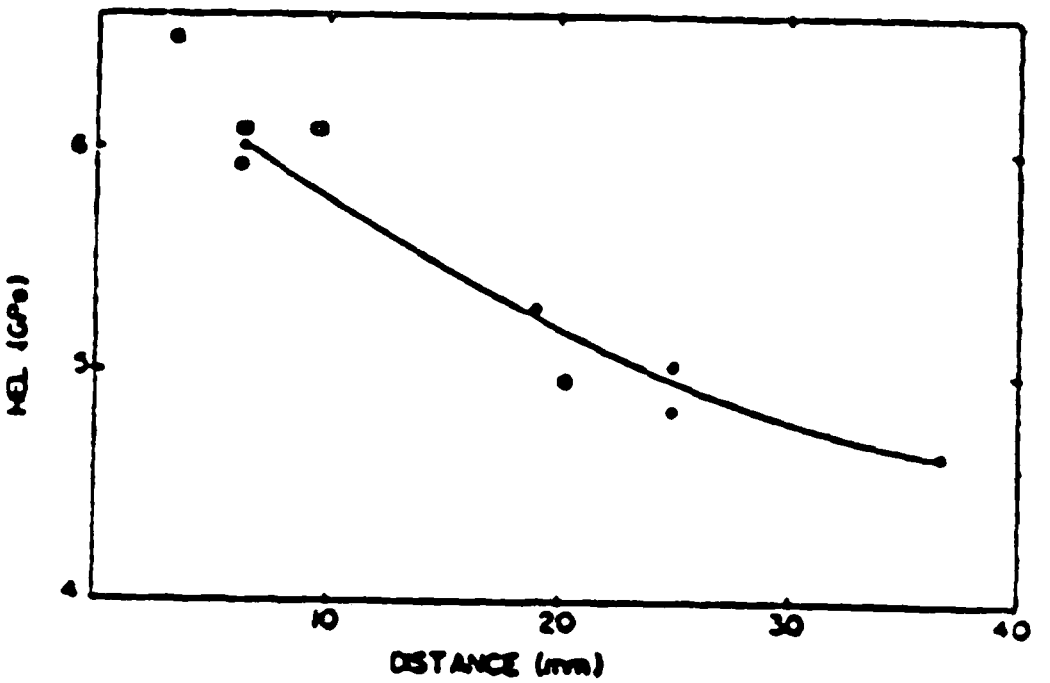

Figure 7. Precursor decay in AD-85 alumina. [20]

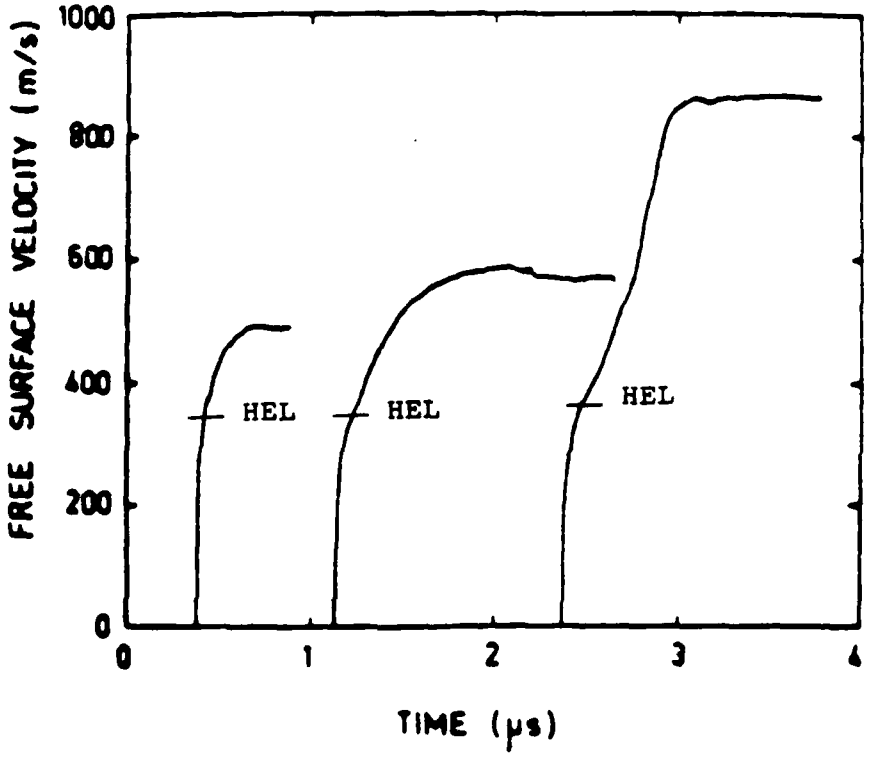

Figure 8. Free surface velocity profiles for Desmarquest alumina. [21]

the properties of the damaged materials. To study the aforementioned properties, more advanced impact experiments have been developed recently. The oblique plate impact experiment shown schematically in Figure 9 and the double flyer plate impact experiment shown in Figures 10a and 10b are two configurations that can be used to evaluate the pressure-shear response and the properties of the damaged material, respectively.

3.1.2.1 Oblique Plate Impact Experiment

As shown in Figure 9a, the configuration of an oblique plate impact experiment is one in which a flyer plate (impactor) impacts a target plate at some predetermined obliquity. The impact generates two waves which propagate away from the impact face. The first is a uniaxial strain compressional wave similar to the wave generated in a normal plate impact experiment. This wave is followed by a slower moving shear wave which propagates into the already compressed material. The normal (pressure) and transverse (shear) velocities on the rear surface of the target are recorded with a pair of velocity interferometers. From these velocity components, the constitutive behavior of the target material can be inferred.

The oblique plate impact experiment has not yet been used to study the behavior of ceramics, it is nonetheless a configuration which can be used to evaluate the pressure-shear interaction along with other shear-related processes (i.e., the effect of shear on spall, compaction of pores, etc.).

3.1.2.2 Double Flyer Plate Experiment

A recently developed experimental technique to evaluate the history effects on material behavior involves impact on a target plate with two flyer plates as shown in Figure 10a. The two flyer plates are separated by a small air gap. The first flyer plate causes spall in the target depending

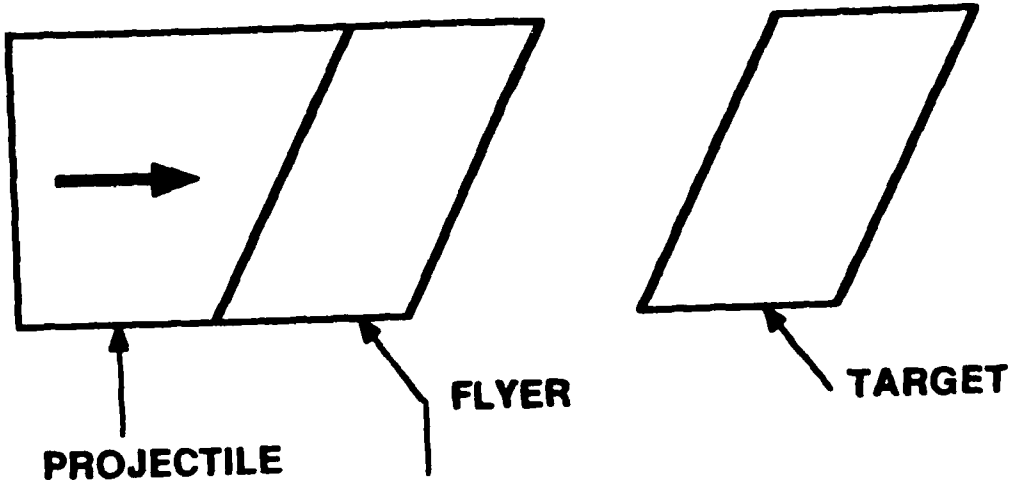

Figure 9. A schematic of oblique impact on combined pressure-shear loading experiment.

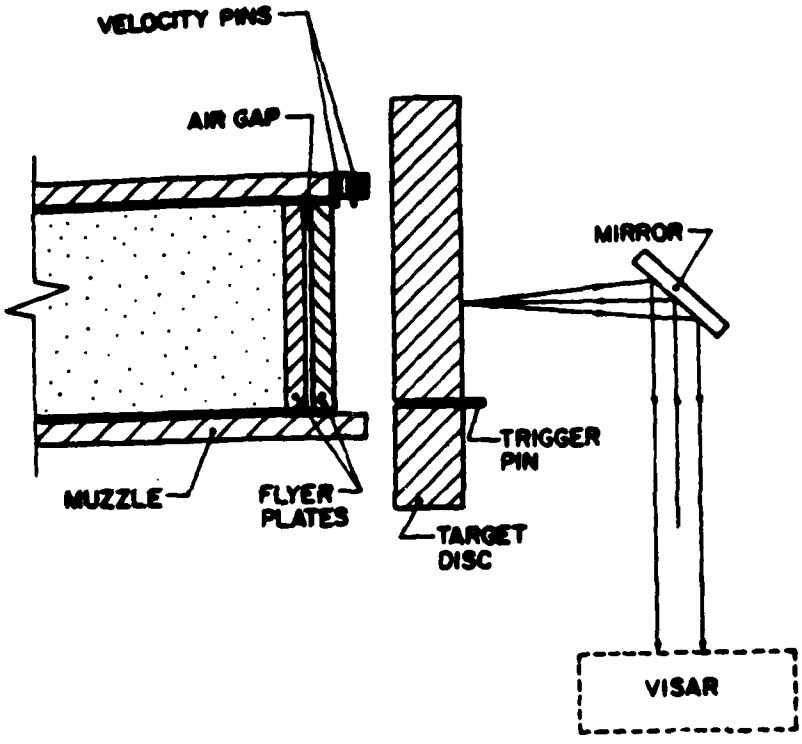

Figure 10a. A schematic of double flyer plate impact (reshock) test.

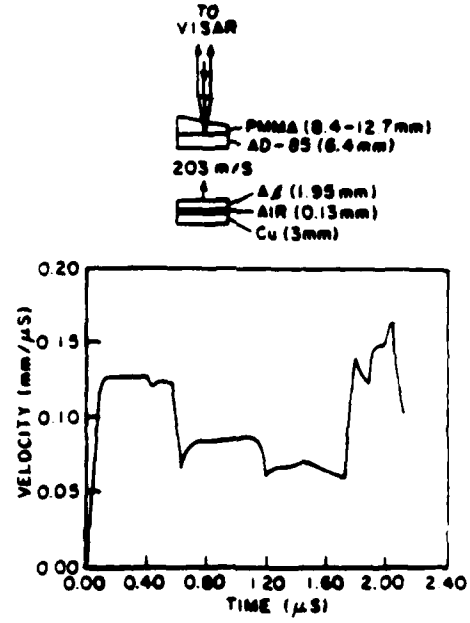

Figure 10b. Typical VISAR signal of the free surface velocity history from the double flyer plate test.

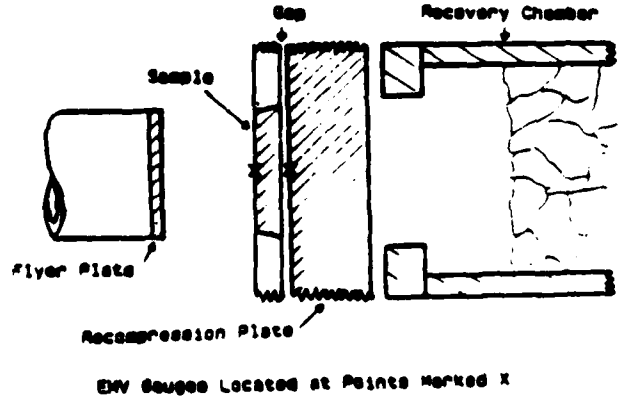

Figure 10c. A schematic of another version of a reshock experiment.[23]

on the impact velocity, and the second plate recompacts the material and allows the determination of the properties of the damaged zone. Yaziv [Reference 22] developed this technique to investigate shock fracture and recompaction of Al300 and AD-85. The particle velocity history at the free surface of AD-85 due to double flyer plate impact is shown in Figure 10b. Since the impact velocity in this case is below the HEL, it is not possible to evaluate the effect of reshocking or recompression on the HEL. However, the recent double flyer plate impact results of Cagnoux and Longly [Reference 21] on fused silica showed this effect as shown in Figure 11. The HEL in silica apparently increased due to shocking.

In principle, the double flyer plate impact technique can be used to extract the properties of fractured materials. Several versions of such recompaction experiment are available. The tension-recompression experiment of Majewski et al. [Reference 23] is another example. In this experiment, the normal plate impact configuration is slightly modified by placing a small gap followed by a recompression plate behind the rear surface of the target as shown in Figure 10c. The few reported results have not yet completely explored this technique for characterizing ceramic materials. A better interpretation and use of these experimental data will require rigorous modeling efforts through computer simulation of the experimental configuration.

3.1.3 Plate Impact Recovery Experiment

Understanding the microstructural characteristics of the deformation and fracture processes due to impact under uniaxial strain conditions requires recovery of the target material. The idea behind the recovery experiment is to prevent the release waves from the lateral surfaces from destroying the uniaxial strain condition in the target. Yaziv [Reference 22]

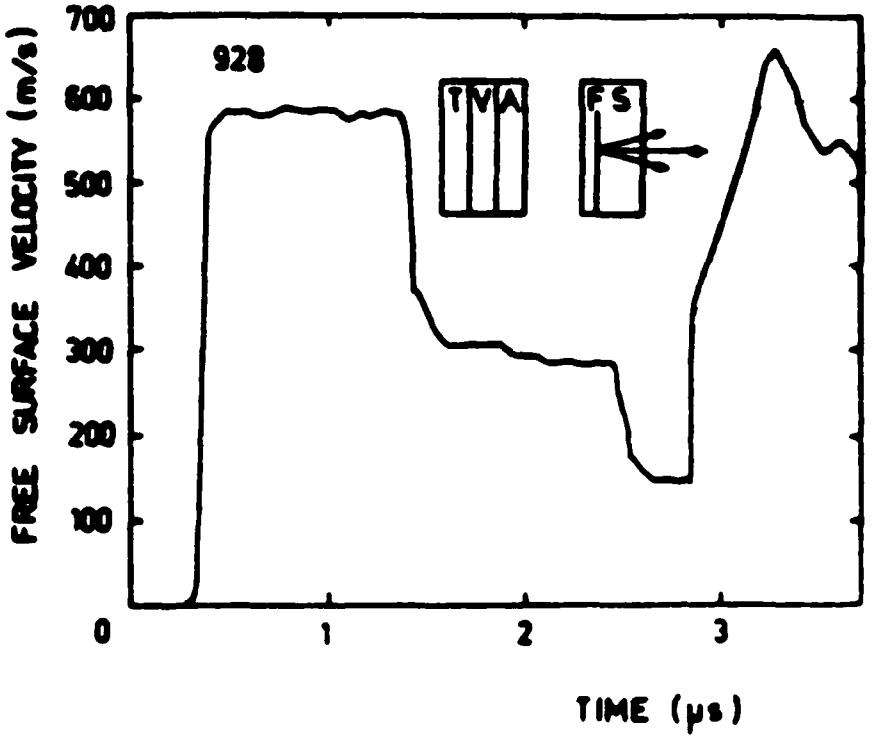

Figure 11. Particle velocity profile in fused silica target. [21]

performed a few recovery experiments on AD-85. The test configuration is shown in Figure 12. In this configuration, a star shaped flyer plate impacted a target plate whose diameter was smaller than the flyer plate. This target was clamped around its lateral edges by a steel ring whose shock impedance was very similar to AD-85. A long catch pipe filled with foam and soft rags was mounted at the back of the target. Yaziv [Reference 22] has described this recovery configuration in detail.

Such recovery tests will be very useful to understand the micromechanics of the deformation and fracture processes. Understanding of the micromechanics will aid in the formulation of appropriate constitutive and failure models. We will explore this aspect of ceramic modeling later.

3.1.4 Split Hopkinson Bar Experiments

A Split Hopkinson Bar (SHB) apparatus generally consists of three bars: a striker bar, an incident bar, and a transmitter bar. The striker bar is made to impact end-to-end onto the incident bar, producing a compressive stress wave in the incident bar whose duration is twice the acoustic transit time of the striker bar. The specimen is placed at the other end of the incident bar, between the incident bar and transmitter bar as shown in Figure 13. The striker, incident, and transmitter bar are all made of the same material and have the same diameter. In order to avoid wave interactions during the test, the lengths of the striker, incident, and transmitter bars are approximately in the ratio of 1:2:2 for a compressive system, and 1:4:2 for a tensile system. For a compressive system, the compressive stress wave that travels down the incident bar is partially transmitted and partially reflected at the specimen. The reflected and transmitted stresses are measured by strain gage stations approximately one striker bar distance from either side of the specimen, and these strain gage signals provide load and displacement rate histories of the specimen. Detailed discussions

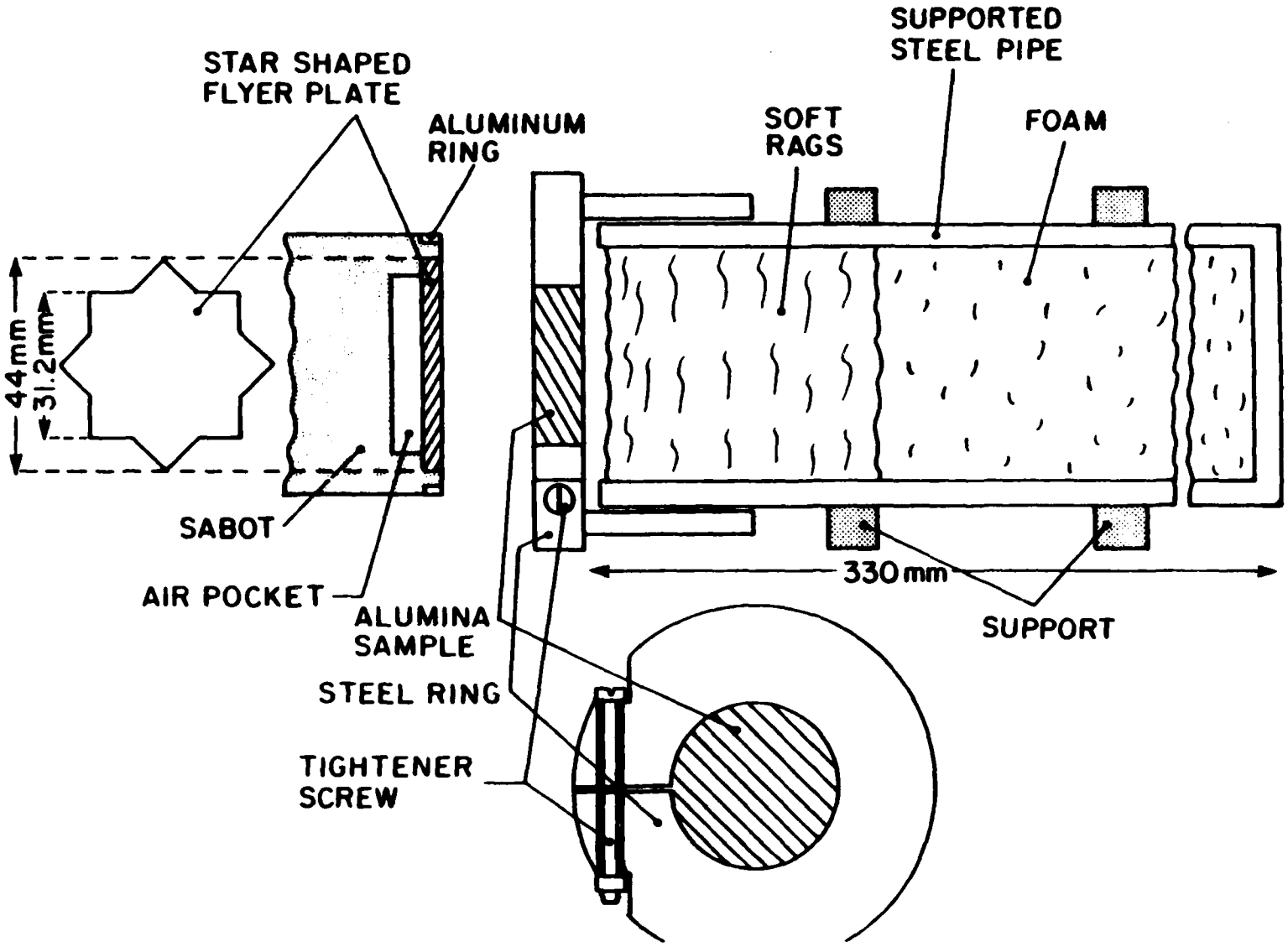

Figure 12. Experimental arrangement for soft recovery of spalled alumina specimens.[22]

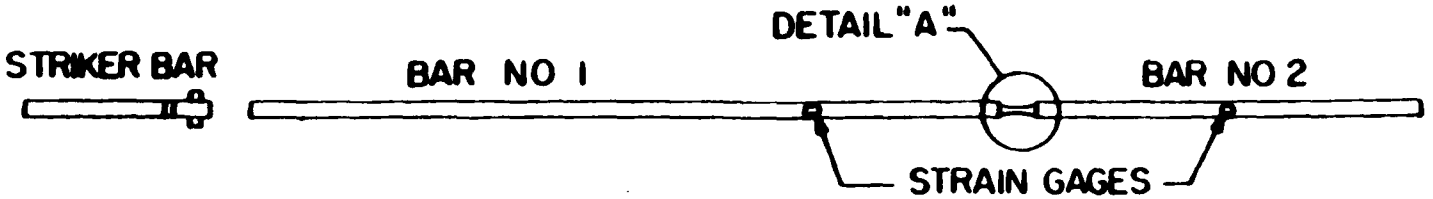

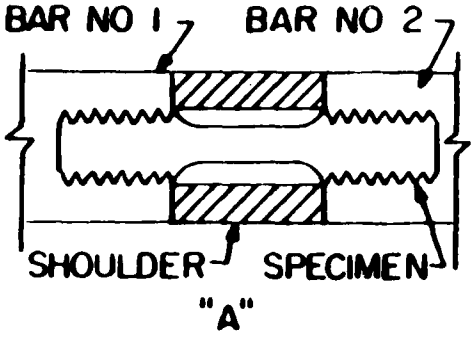

Configuration for a tensile specimen.

Figure 13. Schematic sketch of the SHB setup.

on the strain gage analysis are discussed by Nicholas [Reference 24] and Lindholm [Reference 25].

Usually the SHB apparatus is used to obtain stress-strain curves under both tension and compression for ductile metals at high strain rates (from 100 to 2000 in/in/second). However, the use has been extended to brittle materials, such as concrete [References 26,27] and ceramic [References 28,29]. Lankford [Reference 29] conducted compressive tests on different ceramics and determined the compressive strengths at various strain rates as shown in Figure 14. The compressive strength increased with increasing strain rates for these materials. Use of SHB tests to evaluate ceramic strengths at high strain rates is not frequently reported. Since the recorded strains in the gages due to brittle material deformations are relatively low compared to ductile metal deformation, the accuracy and interpretation of the data require extreme caution. Specimen size relative to the bar size itself plays a key role in trusting the data, and hardened wafers used to protect the generally lower strength steel bars from damage can interfere with the results.

3.1.5 Flyer Plate - Impact on Long Rod

Rosenberg et al. [References 30,31] and Kuscher et al. [Reference 32] reported the use of an experiment to measure initial yield strength in ductile materials at strain rates from 100 to 1000 in/in/second. In this experiment, as schematically shown in Figure 15, a heavy flyer plate impacts one end of a long rod whose length is at least ten times its diameter. The stress state in the long rod away from the impacted end is uniaxial. To measure the stress history in the rod, Rosenberg et al. [References 30,31] embedded a manganin gage at a distance 83.3% of the way down the rod from the impacted end. They measured the initial yield strength for C1008, HY100, and 1020 steels.

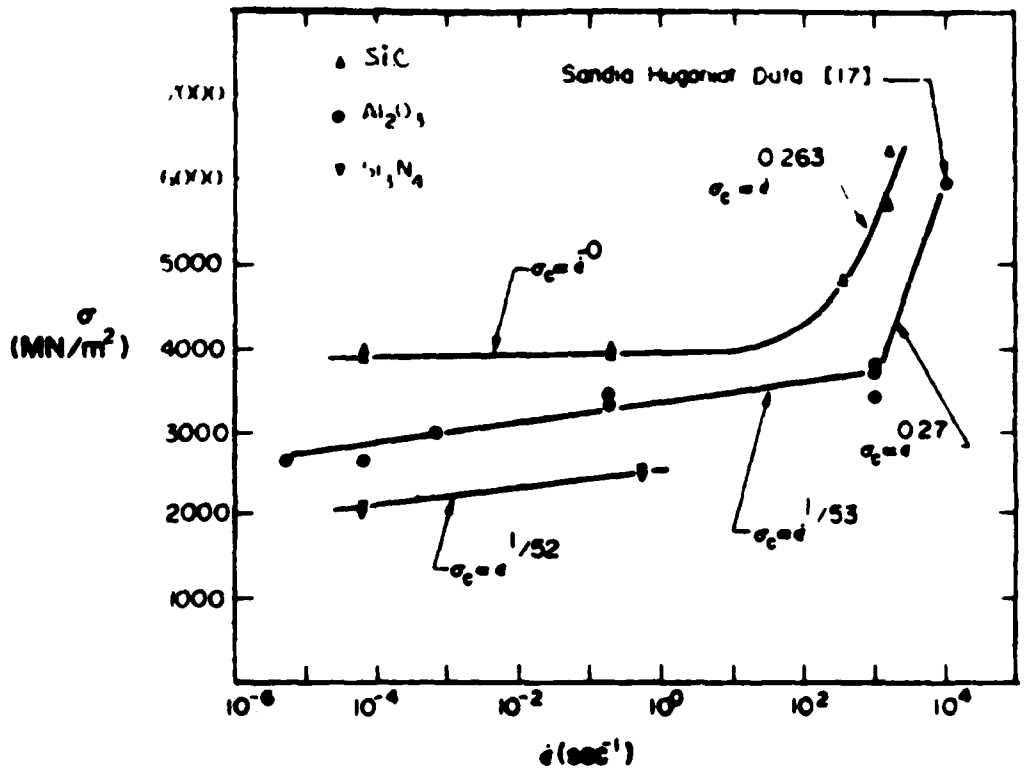

Figure 14. Compressive strength vs. strain rate for Al_2O_3, Si_3N_4, SiC. [29]

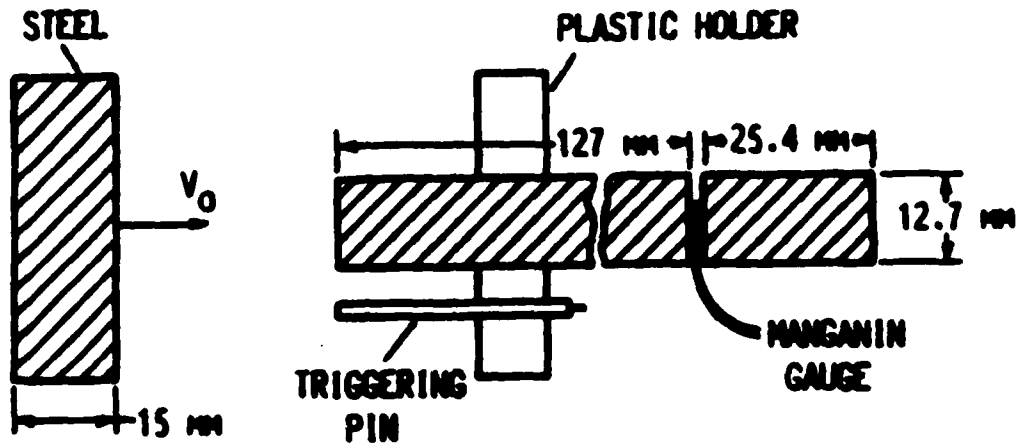

Figure 15. Schematic diagram of long rod experiment.

A sample manganin gage stress history for C1008 steel is shown in Figure 16. The elastic wave arrives at the gage location at point A in the figure. The amplitude reaches its peak value at B (initial yield stress) and remains constant until the arrival of an elastic release wave (point C) from the free end of the rod. Rosenberg and Bless [Reference 31] determined the initial yield strength for C1008, HY100, and 1020 steels from the peak amplitude of the elastic wave from long rod experiments.

The use of long rod experiments has recently been extended to ceramics by Brar et al. [Reference 33]. Figure 17 shows the stress histories from three different tests on AD-99 (99.8% Al_2O_3) ceramic. The velocities in these tests were 102, 160, and 551 meters/second, respectively. At a velocity of 551 meters/second, the release wave from the fracture front (near the impact end) catches up with the elastic wave and allows no time for the elastic amplitude to reach its peak value as can be seen in Figure 17c. When the impact velocity was lowered to 160 meters/second, a similar trend was observed from the gage signal as shown in Figure 17b. However, the peak stress level was lower than the signal at the higher velocity. This may be speculated to be the combined effects of strain rate and confining pressure. The stress gage signal at an impact velocity of 102 meters/second showed a stable elastic stress curve. The peak stress was sustained in the gage until a release wave reached the gage from the free end of the rod (just as it was for metals). This indicates that the release wave from the fracture surface (near the impacted end) did not arrive at the gage section. The average peak value is between 18 and 20 kilobars as shown in Figure 17a. Interestingly, the uniaxial compressive strength obtained from this low velocity test compared well with the quasi-static strength of 20 kilobars for AD-99. These long rod impact tests indicate that the drastic strength increase in ceramic may be due

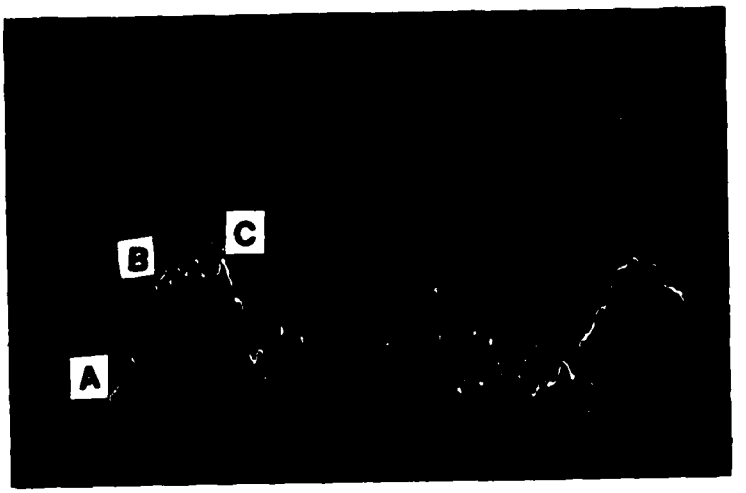

Figure 16. A typical gage record from a long rod experiment, experiment No. 925. [31]

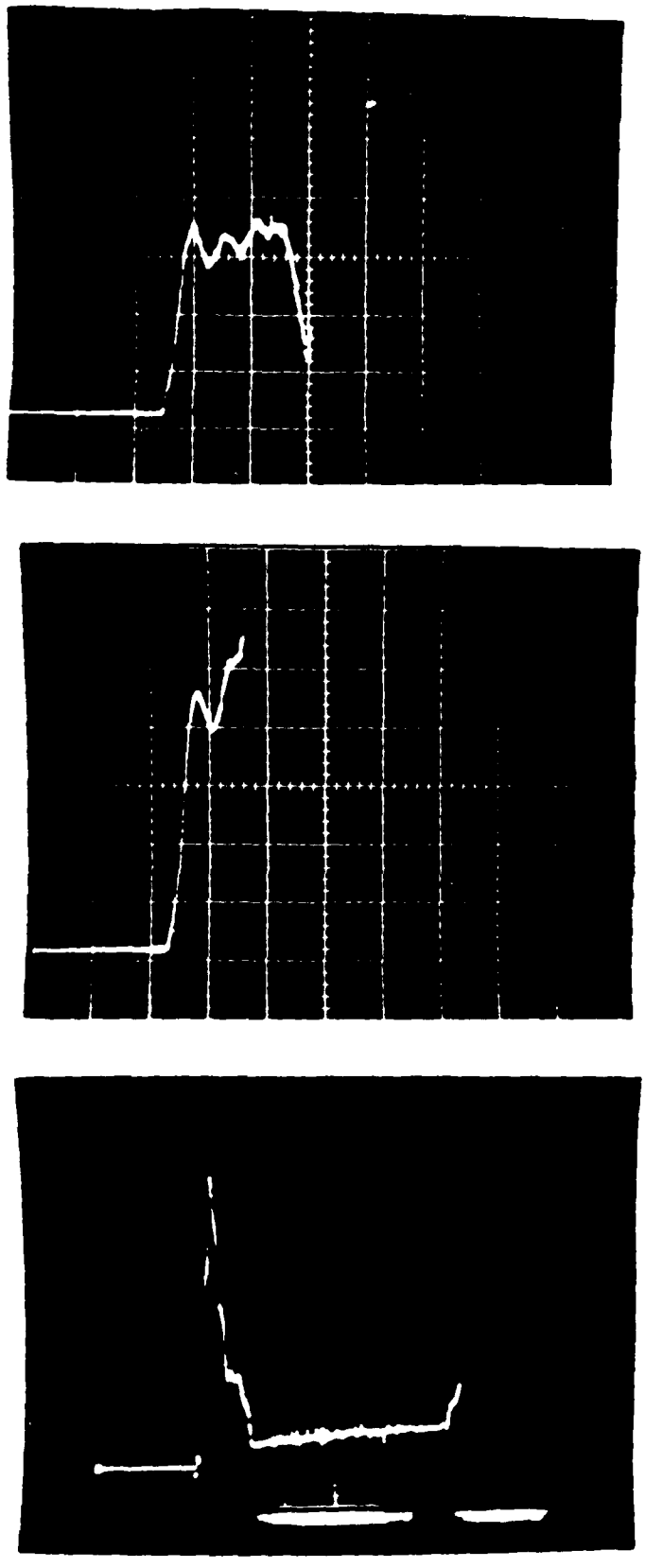

Figure 17. Oscilloscope records from experiments on AD-998 rods. Scales for all records are 0.2 V/div., and 5μs/div. [33]

to both the strain rate and confining pressure. In fact, the earlier mentioned high strain rate test results on alumina as reported by Lankford [Reference 28] support this indication (effect of strain rate).

3.1.6 Penetration Experiments

Wilkins et al. [References 34,35] performed impact and penetration experiments on thin ceramics both with and without confining materials to obtain information on the impact resistance of various ceramic systems. Observations were made on both the performance of different materials and different geometries. Mayseless et al. [Reference 36] have performed a set of similar experiments recently, including more than 150 tests with the objective of "[providing] reliable data on the ballistic performance of the ceramic targets and the projectile erosion in order to create a basis for the development of an analytical model of the process." This work repeats and extends some of Wilkins earlier work, concluding that for thin confined ceramic plates impacted at velocities below 250 meters/second a simple metal plate is more effective at resisting penetration from hardened, pointed penetrators while above 250 meters/second a single confined ceramic plate is more effective. As indicated by the results, tests such as these are better at providing relative measures of impact resistant capacities of ceramic than at developing an understanding of these capabilities. Furthermore, rather than establishing a model that can be derived from physical principles, these tests are more likely to provide empirical models of impact and penetration performance. Based on the assumption that the work of erosion equals the product of the yield strength and the volume of the target removed and an assumed particle size distribution for the fractured ceramic, they conclude that, "the fracture of the ceramic consumes a negligible amount of energy compared to that required for erosion....". A simple model for penetrator erosion is presented assuming no wave

propagation, a linear momentum loss of the projectile during penetration, and a force history derived from displacement measurements. This modeling appeared accurate in the lower velocity range of their work.

Recently, innumerous penetration experiments are conducted in various national and other research laboratories on several difficult ceramic targets with and without any confining materials. These unpublished investigations are routinely conducted to evaluate ceramics for their ballistic performance. A parametric study to determine the most important property of ceramic for its ballistic performance include properties, such as the fracture toughness, HEL, spall strength, hardness, etc. The sizes of the target plates also play significant role in the performance of ceramic materials.

3.2 CERAMIC FAILURE MECHANISMS

There are two distinct categories of failure mechanisms commonly referred to in the literature dealing with impact failure of ceramics, namely microscopic and macroscopic failure mechanisms. The category of failure mechanism most often referred to in the fracture literature is the microscopic failure due to microcrack nucleation, growth, and coalescence, and microplasticity that occurs at the micro crack tips. The other category of failure mechanism is macroscopic in nature and is most often used in the literature dealing with mechanics of penetration. It considers gross structural failure, such as plugging, spallation, fragmentation, and complete pulverization. Modeling of the micromechanisms requires a thorough understanding of the microscopic failure processes that lead to these different modes of failure. The macromechanisms might be appropriately considered as failure modes determined by the geometry as well as the underlying micromechanisms.

Establishing the microscopic failure mechanisms in ceramic materials at high velocity impact loading conditions requires sophisticated recovery techniques and post-impact microstructural studies of the ceramic specimens or targets. Yaziv [Reference 22] attempted to recover AD-85 and AL-300 targets using the star shaped-flyer plate technique [Reference 23]. His study was mainly intended for recompaction of ceramics as well as the evaluation of properties of damaged ceramics. Yaziv did not conduct any rigorous microstructural studies for evaluating any micromechanics behavior. However, such recovery techniques, in principle, can be used to recover the shocked ceramic for further microstructural studies.

Most studies on brittle fracture have considered rock type materials [References 37-42]. In these studies, the micromechanisms of macroscopic failure of rocks are described by nucleation, growth, and interactions of microcracks. According to the microscopic observations, the sites for nucleation include: pre-existing flaws, grain boundaries, interfaces of two different materials (matrix and the second phase particle), and pre-existing micropores. Extension of many of these microscopic mechanisms of rocks to describe ceramic materials is speculative in nature. Until recently, there has been very little physical evidence to describe the mechanisms in ceramic materials under high strain rate loading conditions. It mostly remains speculative, because the recovery of ceramics at high velocity impact is extremely difficult due to catastrophic ceramic failure from low level tensile stresses. Elimination of reflected tensile stresses from the lateral and rear free surfaces is extremely difficult in an impact recovery experiment at high velocity. At extremely high velocities, ceramic completely pulverizes and recovery of the shocked ceramic for microscopic studies is not possible. At low velocities below HEL, however, ceramic deforms elastically only and therefore many of the failure mechanisms

will be absent. Thus establishing clear physical evidence of the microscopic failure processes in ceramics under high velocity impact loading conditions requires even more carefully designed recovery experiments. Intuitively it appears that several of the quasi-statically observed mechanisms can be employed in failure model formulations.

A significant amount of research (see for example [Reference 43]) has been done to evaluate the behavior of several ceramic materials under quasi-static loading conditions. This research involved extensive microstructural analyses. Presence of dislocations near the microcrack tips has been frequently reported [Reference 44] in permanently deformed ceramics. Often the word "plastic" is used to describe the permanent deformations. The term "plastic" is used in two ways. The prevailing use of this word in the ceramic literature implies that any observed non-linear, permanent deformation behavior in the load-deflection or stress-strain response is termed as "plastic". It does not necessarily mean that this inelastic (non-linear) response is due to dislocation motion or twinning based plastic deformations. In contrast, when the word "plastic" is used in a microstructural sense (based on the metallographical studies), it usually implies that plasticity is due to dislocation motions.

Among the most significant recent research on ceramic, Marsh [Reference 45] showed that glass flows plastically under indentation testing. Occurrence of plastic flow at the local indentation sites has been reported by several investigators [Reference 46,47]. Hockey [Reference 47] reported networks of dislocations related to shear cracks. The indentation sites became the favorable sites for the nucleation of shear cracks due to high triaxial stress state under compression. Similar observations of plasticity in brittle materials, based on the transmission electron micrographs of dislocations within the plastic zone, have been reported [Reference 48].

The use of the word "plasticity" to describe the inelastic deformations in ceramics or rocks is mainly based on the extensive applications of metal plasticity theories to concrete materials. Many investigators [References 49-52] describe brittle materials as elastic-plastic solids and employ plasticity based theories. In a plate impact experiment with a ceramic target, the stress history measured using a manganin gage at the interface of target and a back-up plastic plate is usually described by elastic and plastic waves as shown in Figure 18. The initial straight (linear) portion of the stress-time plot from A to B is due to elastic deformation. The curving (ramping) portion of the curve between B and C indicates some kind of inelastic deformation which may be due to microplasticity and/or microcracking. Often, in literature this protion of the curve is called 'plastic'. It is simply a mechanistic use of the word to describe the non-linear, loading path dependent permanent deformations. The stress is released elastically at point C' due to the release wave arrival from the flyer plate.

The use of the word 'plastic' can imply both microcracking and dislocation based inelastic deformations. The dislocation based deformation in ceramics appears to be highly localized as a result of microplasticity at the crack tips rather than full field plastic flow. Constitutive and failure model formulations require proper interpretations of the processes involved and the extent to which they dominate the inelastic response of the material. Based on any metalographical study, if the inelastic deformation of brittle materials is due to "gross" microplastic flow, the model formulation can be within the framework of plasticity theories. When the inelastic deformation is entirely or mostly due to microcracking (nucleation and growth of microcracks), the models must incorporate fracture mechanics based laws and theories for realistic descriptions of inelastic strains under compression.

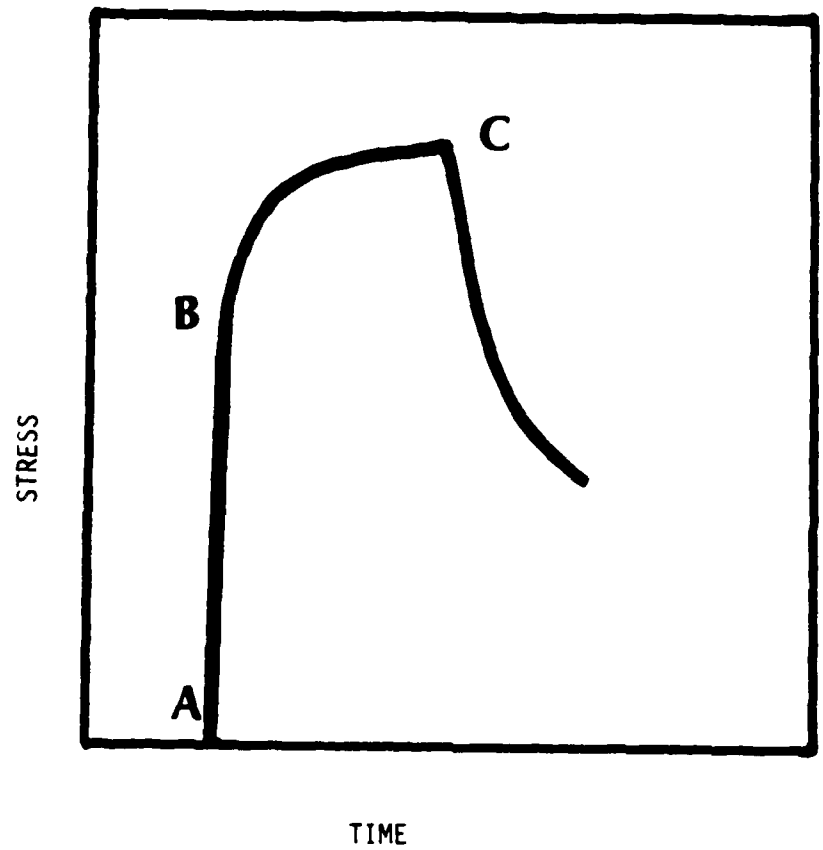

Figure 18. A typical stress history plot in a plate impact test on ceramics.

3.3 MODEL FORMULATIONS

Under static loading conditions, the deformation of ceramic is elastic. Therefore, the stress-strain behavior is described by the Hooke's law based elasticity equations. However, under high velocity impact loading conditions, ceramic materials are often known to exhibit inelastic deformations. In Section 3.2, several phenomena characteristic of the response of brittle materials have been identified with the deformation and failure mechanisms. The theoretical basis of any model should incorporate the various identified phenomena. However, for engineering calculations, it is possible to use simplistic models that do not consider the failure mechanisms explicitly. Such an approach has been often employed for metals. The simplistic models, in an ad hoc manner, include empirical equations based on a few experimental data. For instance, in computer code calculations, failure under negative pressure (tension) is treated simply by setting stresses equal to zero when pressure (P) reaches a small value (PMIN). The brittle ceramic is assumed to have failed abruptly at P = PMIN. This approach does not recognize any microphysical process that contributes to the failure of the material element. Therefore, a sound theoretical basis is obviously not present.

Five distinct approaches can be identified as theoretical basis for describing the inelastic deformation and fracture in brittle solids. In the first approach, the material is assumed to be elastic and stresses are calculated based on Hooke's law equations. Failure is then predicted using a generalized Griffith [References 53,54] fracture criterion.

In the second approach, the material is assumed to behave as an elastic-plastic solid. This approach ignores the details of crack growth and concentrates on describing the effects of localized fracture on stress wave propagation. The concepts and equations are the same as those derived for metal plasticity. As

mentioned earlier, some evidence exists in support of the use of plasticity based equations to describe ceramic like brittle solids. Strain rate dependency is introduced into the ceramic failure models through viscoplastic constitutive equations. For pressure dependent deformations and failure processes, a yield function that depends on the second invariant of the stress deviators, pressure, and damage (crack density, void volume etc.,) is employed. This approach is widely used to describe the inelastic response of concrete materials.

In the third approach, fracture mechanics based microphysical theories and models are employed to describe the deformation due to the compressive failure processes. The basic idea of a microphysical model is to describe the apparent inelastic behavior while keeping track of the microstructural evolutions under a given set of loading conditions. For instance, the damage evolution can be identified with nucleation of cracks/voids and their growth. The description of the damaging processes requires laws/theories that suitably reproduce the observed physical mechanisms. For ceramics, the evolution laws for microcracking must incorporate the fracture mechanics theories that describe the conditions for crack growth. A statistical description of number of cracks per unit volume as a function of position, crack size, and orientation, is an example of a microphysical based approach. In this approach the Hooke's law based elasticity equations are combined with an effective moduli description that relates the microstructure to the macroscopic material properties.

In the fourth approach, microstatistical based fracture models that embody several of the phenomenological concepts derived from the microstructural evolutions, are considered. The theoretical formulation does not necessarily incorporate fracture mechanics and continuum damage mechanics based equations and theories. Based on the experimental observations which involve

extensive microstructural analyses, phenomenological laws are usually formulated. Deduction of a suitable statistical distribution of the evolution is an important part of this approach. The damage evolutions in terms of microcrack nucleation and growth are modeled using empirical or intuitive equations which relate pressure, temperature, and internal energy, or any other state variables.

In the final (fifth) approach, constitutive and failure equations are based on the theory of continuum damage mechanics. In this theory, the constitutive equation for the stress or strain is derived from either Helmholtz or Gibbs free energy density functions. These constitutive relationships are subjected to the restrictions imposed by the second law of thermodynamics. Damage laws/equations are usually postulated based on a phenomenological approach. Sometimes, these laws can also be formulated from microstatistical analyses of the actual fracture processes.

In summary, a combined features of these various approaches is often found in modeling of brittle material behavior. It is usually difficult to classify a model under one particular approach. For example, nucleation laws in a model may follow microstatistical approach while the stress-strain relationship is based on the continuum damage approach. Therefore, in the following section, the various models described for brittle solids do not necessarily fall uniquely under only one of the five approaches. However, one model may incorporate concepts and equations from several approaches.

3.4 MODELING

Several constitutive and failure models that describe deformation and fracture in brittle materials are reviewed below. No attempt is made to include modeling under high temperature creep or quasi-static cyclic loading conditions. Fracture

mechanics based models which describe slow crack growth or the models which describe the effects of temperature, strain rate, and environment on the fracture toughness (K_{Ic}) properties are not considered. Only models which are applicable and extendable to describe ceramics under impact loading conditions are considered. While describing the models, the salient features are pointed out without elaborate mathematical details.

3.4.1 Simple, Instantaneous Models

Simple models assume that failure occurs instantaneously when stress, strain, energy, or any other state variable reaches a critical value. The deformation processes are described by elasticity equations. No attempts are made to identify any microphysical aspects of deformation and failure. Preliminary evaluations of new engineering design concepts (fabrication of mining and tunnelling, armor, penetrator, meteoroid impact on space structures etc.,) often involve the effective use of this approach in computer code calculations. Wilkins [Reference 55] in his computer calculations of a sharp steel projectile penetration into a ceramic armor, employed this approach. A critical strain based instantaneous failure criterion was used in the calculations.

The reason for mentioning this simple approach is to recognize the fact that such calculations, though they are not based on physically based rigorous material models, can provide an approximate and quick engineering estimation of the solution to certain impact problems. However, further validation of such predictions may require extensive experimental verifications. Indiscrete use of simple models to solve complex impact problems may lead to erroneous results. Under such circumstances, improved understanding and better descriptions of ceramic materials will be essential.

3.4.2 Plasticity Based Models

Plasticity theory based constitutive and failure model descriptions for brittle materials provide an alternative and improved approach in code calculations. This approach has been successfully employed by several investigators (Wilkins [Reference 55], Glenn [Reference 56], Wilkins [Reference 57], Glenn [Reference 58]). It is widely used in explosive loading analyses of armor, oil shale, fragmentation of rocks, concrete structures, etc.

Wilkins [Reference 55] described several ceramics as elastic-perfectly plastic solids in his light armor design analyses. Ceramic is assumed to be elastic when the effective stress (equal to J_2, the second invariant of the deviatoric stress tensor) is related to the yield strength (Y_o) as indicated below:

$$3J_2 \leq Y_o \qquad (2)$$

Y_o may be either the compressive or tensile strength at high strain rates. The value of Y_o is determined from plate impact experiments since it is related to HEL through Equation 1. Glenn [Reference 56] presented his calculations of brittle fracture in rock-like media. Elastic-plastic constitutive models with and without plastic dilatation (plastic compressibility due to voids) were used to describe the inelastic deformations. Dilatation effects were considered because of the porosity. Glenn used the generalized Mohr-Coulomb criterion for describing the failure surface. The failure surface was defined by:

$$J_2 = (f(P))^2 \qquad (3)$$

again J_2 is the second invariant of the stress tensor and P is given by:

$$P = 1/2(\max \sigma_i + \min \sigma_i) \quad (4)$$

where σ_i are the principal stresses. The brittle fracture in several types of rocks (limestones, granites) and ceramic materials (pyrex glass) was modeled using the above criterion. Failure of the material is assumed in the code calculations when $\sqrt{J_2}$ equals f(P). Glenn's definition of failure is the initiation of inelastic deformation due to either microcracking or plastic flows. The stress-strain relationship is elastic (Hooke's Law) until the failure criterion is met and beyond this the material is assumed to be plastic. The material is then modeled based on plasticity theories. Glenn [Reference 58] used this approach to model the impact behavior of glass. Fracture under compression is not considered. A similar elastic-plastic approach was used by Taylor et al. [Reference 41] and Grady and Kipp [Reference 39] in their analyses of brittle failure in oil shales.

3.4.3 Nucleation and Growth Models

Nucleation and growth models have been developed extensively over the past 20 years, predominantly by Curran et al. [References 59,60,61]. Most of the work has been for ductile and/or brittle metals. These models are built on the observation of material failures due to the growth of either cracks or voids that nucleate from heterogeneities on the microscopic scale in the solid. Based on the metallographical studies on the recovered targets from the impact experiments, an initial distribution of inherent flaws (inclusions, voids, crazed zones, pile-up dislocations, etc.) is taken as:

$$N_g(R) = N_o \exp(-R/R_1) \quad (5)$$

where N_o and R_1 are the material constants, R is flaw size (radius), and N_g is the number of flaws per unit volume with a grain size greater than R.

A localized threshold for inherent flaws often requires a condition as:

$$F[\frac{\sigma_m}{\sigma_y}, \bar{\epsilon}^p, \dot{\bar{\epsilon}}^p, T, R] \geq 0 \qquad (6)$$

where σ_m is mean stress, σ_y is yield stress, $\bar{\epsilon}^p$ is plastic strain, $\dot{\bar{\epsilon}}^p$ is plastic strain rate, T is temperature, and R is flaw size. When favorable conditions exist for crack nucleation and growth, the description of the nucleation and growth processes, will require appropriate functional forms.

A nucleation rate function is taken to be the sum of three terms, the first a thermal rate diffusion driven nucleation term, the second a term due to mechanical debonding from the plastic strain, and the third a term due to debonding of inclusions due to mean tensile stress.

Following nucleation, microscopic damage features such as voids or cracks grow under continued loading. Growth may occur due to several types of processes such as atomic diffusion, ductile plastic flow, brittle crack extension, or shear slipping and extension. Each may be expressed mathematically in very different forms. For ceramics, brittle crack growth would seem to be the most critical process. However, Curran et al. [Reference 59] considered ductile crack growth in materials, such as the armco iron and beryllium. The corresponding growth law is given by,

$$\dot{R} = T_1(\sigma - \sigma_{g_o})R \qquad (7)$$

where T_1 and σ_{g_o} are material parameters. These microstatistically evaluated nucleation and growth laws (Equations 5 and 7) are usually coupled to a damage parameter. Most often the crack

volume, which is calculated over the entire crack size distribution, serves as the damage parameter.

The final stage of this damage model treats the coalescence of cracks and voids, leading to a prediction of material separation and fragmentation. The microstatistical approach of Curran et al. [Reference 59] is used often to describe fracture in brittle materials under tensile loading. Furthermore, for applications to ceramics, there have been no reported extensions of this model to consider compressive failure processes. However for modeling of fragmentation, this approach provides a methodology and using which estimation of number of fragments can be possibly made.

3.4.4 Fragmentation Models

One of the important failure modes in brittle solids is fragmentation due to severe impact or explosive loading. Estimation of the size and velocity of the fragments is required to evaluate the additional damage that these fragments may create in the surrounding structural elements. Grady [Reference 62] derived a simple model for dynamic fragmentation through an energy balance criterion. The available kinetic energy is balanced against the energy associated with the new surface created from fracturing. The nominal fragment diameter for a brittle solid as derived by Grady is:

$$d = \left(\frac{\beta K_{Ic}}{\rho C \dot{\epsilon}}\right)^{2/3} \quad \text{and} \quad \beta = \sqrt{2\sigma} \tag{8}$$

where K_{Ic} is the fracture toughness, ρ is the material density, C is the uniaxial (stress) wave speed, and $\dot{\epsilon}$ is the applied strain rate. This expression suggests that at low strain rates, the brittle material fractures into large fragments and at very high strain rates it pulverizes completely. When the impact velocity

is such that the shock stress is above the steady state value of HEL, ceramics are in general observed to fracture by complete pulverization.

Glenn and Chudnovsky [Reference 63] rederived Grady's expression by including the elastic strain energy contribution to the energy balance equation. This leads to a slight modification for the value of β. Based on the rederivation, β equals to $\sqrt{5}$. Later Glenn et al. [Reference 64] presented a fracture mechanics model of fragmentation in which they showed that their model permits a unification of previous results, yielding Griffith's solution at the low strain rate limit and Grady's solution at high strain rates.

These fragmentation models are used in the damage model formulations of Kipp and Grady [Reference 65], and Taylor, Chen and Kuszmaul [Reference 41]. To describe tensile damage in terms of crack density, the characteristic flaw size is assumed to be directly proportional to the radius of the average fragment size. Therefore, the expression for fragment size serves as the crack size description in brittle fracture models.

3.4.5 Damage Accumulation Model

Taylor, Chen, and Kuszmaul [Reference 41] proposed a computationally oriented constitutive/failure model (TCK model) to describe rock behavior under dynamic loading conditions. They used the microcrack mechanics approach for tension and the plasticity approach for compression. Recently, Rajendran et al. [Reference 66] adapted this model to describe ceramic behavior under impact loading conditions. The TCK model could be further strengthened by incorporating a description of damage under compression. However, damage is treated as a scalar and in principle, faulting type failure modes cannot be modeled. In summary, the strengths of the model are:

- mathematically simple,
- a few model parameters and direct determination of these parameters,
- easy to implement into computer codes,
- strain-rate dependent, and
- damaged degrades the elastic moduli.

3.4.6 Fracture Mechanics Based Models

Owing to the brittle nature of ceramics, the damage experienced by the material during loading often involves nucleation and growth of microcracks. The microcracks eventually coalesce and form macrocracks leading to failure. For this reason, a fracture mechanics based approach to model microcrack growths in a ceramic seems plausible because it provides a sound theoretical basis for analyzing the cracking process. In this section, the fracture mechanics based models that describe brittle behavior are discussed. Although most of those models were developed to simulate the quasi-static behavior of rocks, it seems that with the proper modifications, the application of these models can be extended to include modeling the dynamic behavior of ceramics.

3.4.6.1 Margolin Model [References 42,54,67,68]

Several models have been developed for quasi-static loading conditions. Most of the fundamental processes that have been modeled under static loading conditions can be suitably extended to describing the damage processes under dynamic loading. Such an approach has been used by Margolin to model the dynamic behavior of rocks under tension and compression. The Margolin model is very appealing due to its relative simplicity. Specific features of the model are presented in Table 2. This microphysical model considers crack opening and sliding under both tensile and compressive loading. The effects of strain rate, pressure, and damage on the compressive strength

TABLE 2

SPECIFIC FEATURES OF THE MARGOLIN MODEL
[References 42,54,67,68]

ELASTIC MODULI FOR CRACKED BODIES

- Micromechanical formulation
- Both tension and compression, including triaxial
- Three-dimensional stress state
- Isotropic or bedded
- No microcrack interactions
- Strain rate dependent

DEFINITION OF DAMGAE (D)

- Scalar quantity assuming random crack orientation
- Calculated under tension and compression
- $D = \int \beta N(a) a^3 da$

  where β is crack geometry parameter
  a is the microcrack size
  N(a) is the statistical crack distribution

MICROCRACK DISTRIBUTION

$N(a) = N_o e^{-a/a_o}$; a_o = characteristic crack size

MICROCRACK GROWTH LAWS

- Mode 2 (shear mode) crack growth
- Generalized Griffith criterion used to initiate crack growth
- Crack extension rate is constant and equal to a fraction of the Rayleigh wave speed
- Growth under both tension and compression

FAILURE CRITERION

- $D = D_{cr}$
- When the relative volume of the microcracks reaches a critical value, the material element has completely failed.

are built into the model. The strain rate effect on the stress versus strain curves as predicted by this model is shown in Figure 19. The effects of strain rate on the fracture stress are shown in Figure 20.

Among the dynamic models reviewed, Margolin's model is the only one that considers microcrack growth under compression. This model addresses crack growth in shear only (mode 2). This sliding mode is due to the frictional forces across the crack faces under compression. The continuum damage based approach is employed which incorporates microcrack growth dynamics in damage evolution. The damage is either isotropic for randomly distributed cracks or anisotropic for bedded crack assumption. In summary, the strengths of this model are:

- dynamic crack growth
- crack gowth under mode 2
- model has been used to describe shock and cratering experiments
- strain-rate dependent damage calculation under both compression and tension
- degradaton of elastic moduli

Although Margolin's model is more sophisticated than the TCK model in describing the compressive behavior of ceramics, it lacks damage induced anisotropic description as those of Costin and Stone [References 69,70] and Horii and Nemat-Nasser [References 71,72,73]. These models were developed to describe the brittle failure under quasi-static compressive loading.

3.4.6.2 Costin and Stone Model [References 69,70]

The Costin and Stone model explicitly considers the microcrack orientation and anisotropic microcrack growth in different orientations. Specific features of this

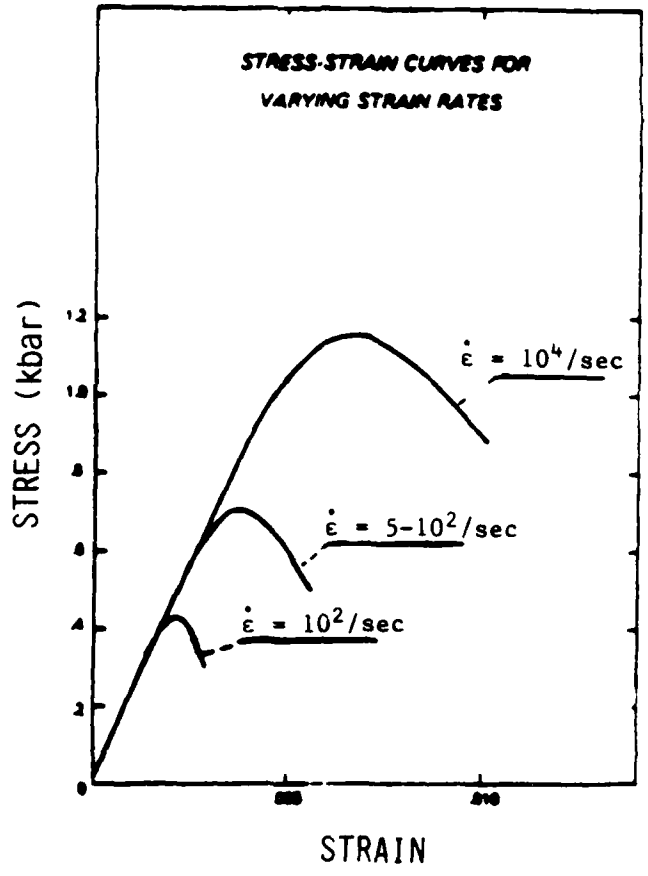

Figure 19. Stress-strain curves for oil shale for three strain rates. [42]

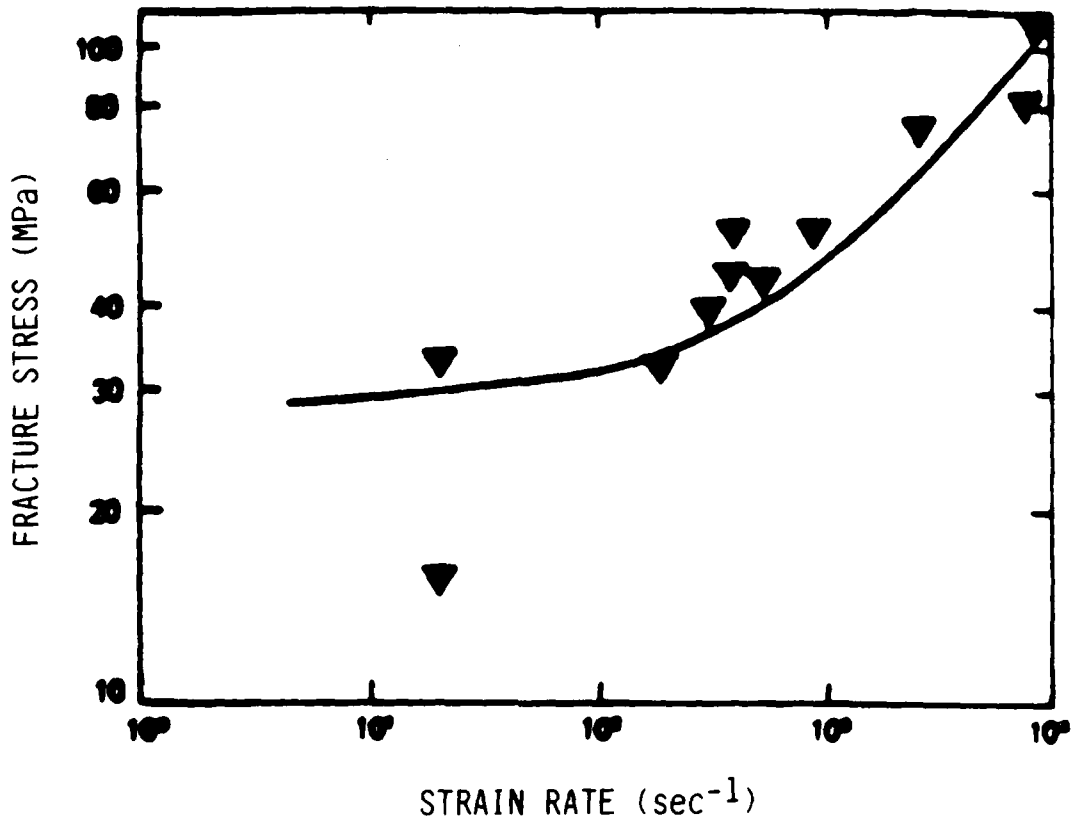

Figure 20. Plot of fracture stress vs. strain rate for oil shale. The triangles are the experimental data of Grady and Kipp. The solid line represents computer simulations with the BCM (Bedded Crack Model). [42]

model are summarized in Table 3. The damage is defined as a vector whose components are in 13 different orientations in two-dimensional problems and 144 directions in three-dimensional problems. Recently, Costin and Stone successfully demonstrated their continuum damage mechanics/LEFM (Linear Elastic Fracture Mechanics) based approach by modeling the deformation and failure behavior in rocks under quasi-static compressive loading [Reference 70]. The effect of confining pressure on the fracture stress and the unloading path is shown in Figure 21. This is an important aspect of their model. The Costin and Stone model is capable of modeling splitting and faulting type failure modes due to its ability to model anisotropic damage. In summary, the strengths of this model are:

- successfully implemented into a computer code (quasi-static)
- demonstrated model capability
- models dilatancy
- describes failure under compression
- includes confining pressure effects
- models anisotropic effects due to microcrack growth
- few model parameters
- methods are available to obtain model parameters.

3.4.6.3 Horii and Nemat-Nasser Model [References 71,72,73]

The constitutive model of Horii and Nemat-Nasser is based on elastic moduli for cracked bodies [Reference 72]. Specific features of this model are summarized in Table 4. The effects of crack opening, sliding, and tearing on the elastic moduli are analytically derived. The microcracks are assumed to be penny shaped and randomly oriented. The stress intensity factor derivations are rigorous and three dimensional. This model treats damage as the relative volume of microcracks.

TABLE 3

SPECIFIC FEATURES OF THE COSTIN AND STONE MODEL
[References 69,70]

ELASTIC MODULI FOR CRACKED BODIES

- Continuum damage mechanics using Gibbs Free Energy function
- Both under tension and compression
- Pressure dependent
- Includes crack interaction effects

DEFINITION OF DAMGAE (D)

- Damage is assumed to be a vector
- Crack opening - Mode 1
- Penny-shaped cracks
- $D_i = \frac{1}{a_o} \int_{\Omega} e_i(\vec{a} - \vec{a}_o)\, H(K_I)\, d\Omega$

  where $\vec{a} - a\vec{n}$; a is the crack size

  n is the unit normal perpendicular to the crack size

  a_o = the initial flaw (microcrack) size

  $(K_I) = 0 \quad K_I < K_{Ic}$

  $= 1 \quad K_I \geq K_{Ic}$

MICROCRACK DISTRIBUTION

$\vec{a}_o = a_o\vec{n}$ where a_o is the initial flaw size as a function of various orientations

MICROCRACK GROWTH LAWS

- $K_I = K_{Ic}$ (static crack growth)

  The estimation of K_I is empirically formulated from the results of Horii and Nemat-Nasser (1985)

FAILURE CRITERION

- Microcrack size reaches a critical value with respect to the microcrack spacings

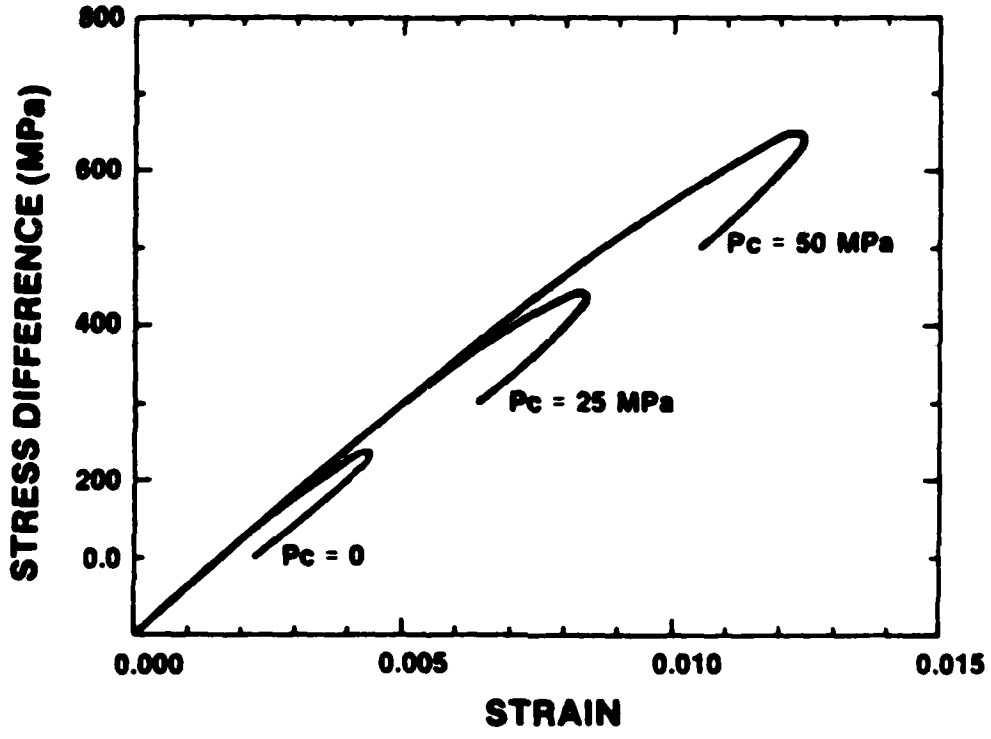

Figure 21. Model simulations of triaxial tests on Westerly granite at different confining pressures ($T_{11}=P_c$). Stress difference is $T_{33}-P_c$. [69]

TABLE 4

SPECIFIC FEATURES OF THE HORII AND NEMAT-NASSER MODEL
[References 71,72,73]

ELASTIC MODULI FOR CRACK BODIES

- Micromechanical formulation
- Isotropic in three-dimensional (tension)
- Anisotropic moduli in two-dimensional under both tension and compression
- Includes crack interaction effects

DEFINITION OF DAMAGE (D)

$$D = \bar{N}\,\bar{a}^3$$

- Scalar function of average number of cracks ($\bar{N}$) and average crack size ($\bar{a}$)
- No description of N
- No attempt to estimate 'a'

MICROCRACK DISTRIBUTION

- No attempt is made

MICROCRACK GROWTH LAWS

- $K_I = K_{Ic}$

FAILURE CRITERION

- Critical ratio of average crack size to crack spacing (STATIC)

The damage is considered to be a single scalar, independent of the orientation of microcracks. No attempt is made to describe microstatistics of crack nucleation process. The microcrack growth is also not considered. This model is developed to calculate the elastic moduli of cracked bodies for which the average number of cracks per volume and the average crack size are assumed to be known.

In recent work, Horii and Nemat-Nasser [Reference 73] have developed a failure model to simulate the experimentally observed failure modes under axial compression, with and without lateral confining pressures. The splitting and faulting type failure modes are successfully predicted by this model. The complexity of the model is due to the stress intensity factor calculations for the tensile cracks that nucleate and grow at the pre-existing, but closed microflaws. While this failure model describes only the final failure process, it can be used to predict the brittle to ductile transition of brittle materials. In summary, the strengths of this model are:

- proven capability in predicting modes 1 (opening), 2 (sliding), and 3 (tearing)
- effects of confining pressure are included
- models splitting and faulting modes of failure
- models brittle to ductile transition.

3.4.6.4 Krajcinovic and Fanella Model [Reference 74]

Krajcinovic and Fanella described the non-linear behavior of brittle concrete under static loading [Reference 74] using continuum damage based constitutive relationships as summarized in Table 5. The elastic moduli description utilizes the micromechanical approach similar to Margolin [Reference 68] or Horii and Nemat-Nasser [Reference 72],

TABLE 5

SPECIFIC FEATURES OF THE KRAJCINOVIC AND FONELLA MODEL
[Reference 74]

ELASTIC MODULI FOR CRACKED BODIES

- Both tension and compression, including confinement
- Three-dimensional stress state
- Anisotropic
- No microcrack interactions
- Micromechanical formulation

DEFINITION OF DAMAGE (D)

- Scalar quantity
- Calculated under tension and compression
- $D = \int_{a_m}^{a_M} \beta P(a) a^3 da$

  where β is crack geometry parameter

  a is the microcrack size

  P(a) is a probability density function for the crack

PROBABILITY - DENSITY FUNCTION

- $P(a) = \frac{n_a}{a_M - a_m}$

  a_m = minimum microcrack

  a_M = maximum microcrack

  n_a = number of aggregates per unit volume

MICROCRACK GROWTH LAW

- Static

FAILURE CRITERION

- None; modeling of softening is not intended

but incorporates recent results of Nemat-Nasser [References 71,73] for describing faulting and splitting of multiple microcracks. The damage variable is treated as a scalar for each phase of crack growth. The treatment is such that the elastic moduli calculations include anisotropy. The damaged moduli calculations require numerical solutions of several double integrals. Also, the anisotropic compliance moduli must be inverted numerically to use in dynamic structural codes. The model is thus computationally complex. Effects of confining pressure can be modeled using this model. Examples are shown in Figures 22 and 23 for concrete behavior under uniaxial and confining compression, respectively. In these figures, dilation due to crack opening in the lateral direction makes the stress-strain curve in the lateral direction non-linear. Due to dilation, the volumetric strain increases to a maximum. A few features of the model is as follows:

- models dilatancy,
- models anisotropic damage,
- includes confining pressure effects, and
- can be extended to dynamic loading.

3.4.6.5 Ilankamban and Krajcinovic Model [Reference 75]

This constitutive model has been developed for describing the non-linear behavior of progressively deteriorating brittle solids under static loading. The modeling approach is within the framework of continuum damage mechanics. A few specifics of this model is briefly described in Table 6. In this formulation, the Helmholtz Free Energy is a function of damage and strain components. Since stress components are derived from this function, the model allows damage to degrade the elastic moduli. Damage is irreversible and its evolution law

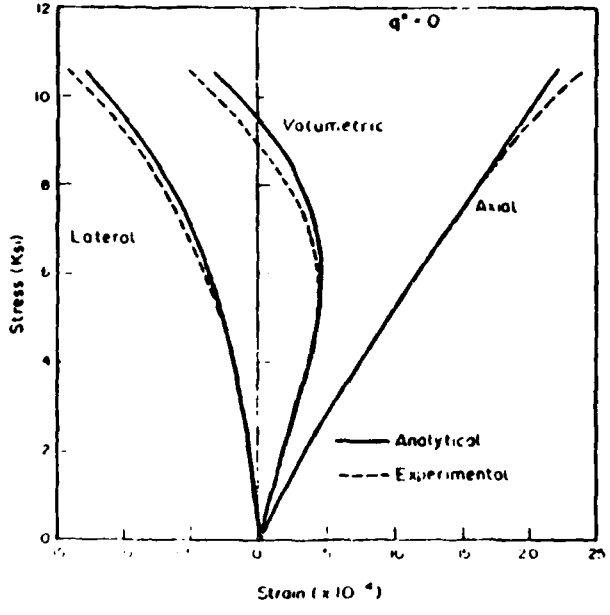

Figure 22. Comparison of the analytical and experimental stress-strain curves for uniaxial compression (unconfined specimen).[74]

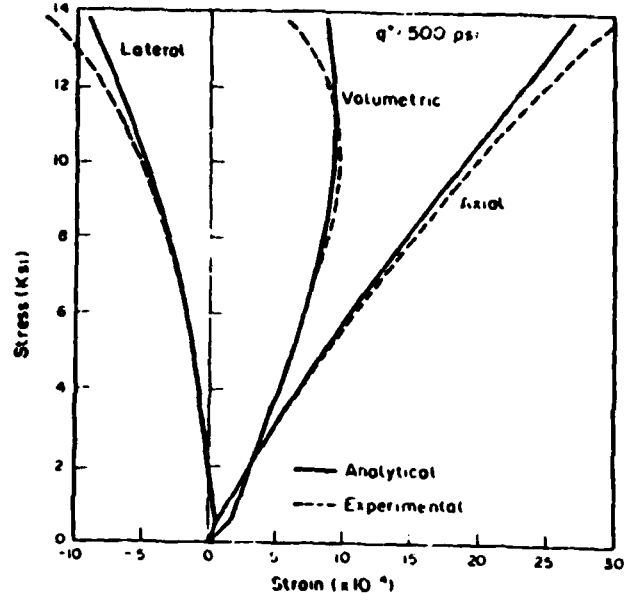

Figure 23. Comparison of the analytical and experimental stress-strain curves for triaxial compression (q = 500psi).[74]

TABLE 6

SPECIFIC FEATURES OF THE ILANKAMBAN AND KRAJCINOVIC MODEL
[Reference 75]

ELASTIC MODULI FOR DAMAGED BODIES

- Continuum damage mechanics (Helmholtz Free Energy)
- Both tension and compression
- 3-D stress state

DEFINITION OF DAMAGE

- No microcrack interaction
- Proportional to vector space of microcrack densities
- Both under tension and compression

MICROCRACK DISTRIBUTION

- Vector space of microcrack density

MICROCRACK GROWTH LAWS

- Damage surface which separates the elastic domain from the inelastic domain
- Microcrack density empirically related to its conjugate thermodynamic force

FAILURE CRITERION

- Not provided

is expressed through an empirical relationship between the microcrack densities and their conjugate thermodynamic forces.

The effect of confining pressure in the model is shown in Figure 24 where it is demonstrated that strength increases proportionally with increasing pressure. The model is able to show the observed trends in the microcrack distributions. Both faulting and splitting modes of failures are modeled. Near failure, the microcrack growth accelerates rapidly over a large range of orientations which lead to faulting. In summary, the advantages of this model are:

- models dilatancy,
- models anisotropic damage,
- includes confining pressure effects,
- includes faulting and splitting under compression, and
- computationally efficient due to the direct derivation of elastic stiffness moduli and a simple damage evolution law.

3.4.6.6 Simo and Ju Model [References 76,77]

A continuum damage mechanics approach using the Helmholtz Free Energy formulation is considered to model anisotropic, rate-dependent brittle and ductile behaviors. The damage evolution law is empirical, but constrained by the application of the first and second laws of thermodynamics. The model formulation requires strain or stress based damage and yield surfaces. The inelastic strain includes the effects due to microcracking and plastic flow. The summary of this model is given in Table 7. The effect of strain rate on the stress versus strain curves is shown in Figure 25. A more general form of either Helmholtz or Gibbs Free Energy functions for describing isotropy, anisotropy, rate independency, rate-dependency, and damage is considered. The confining pressure effects are not

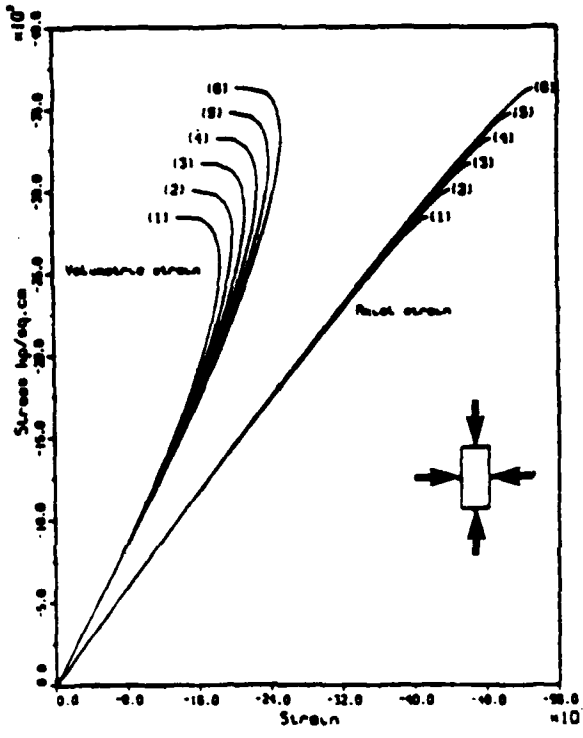

Figure 24. Axial and volumetric stress-strain curves at low confinement pressures for quartzite. Confinement pressure: (1) unconfined; (2) 1% of C_f; (3) 2% of C_f; (4) 3% of C_f; (5) 4% of C_f; (6) 5% of C_f (where C_f is the compressive strength).[75]

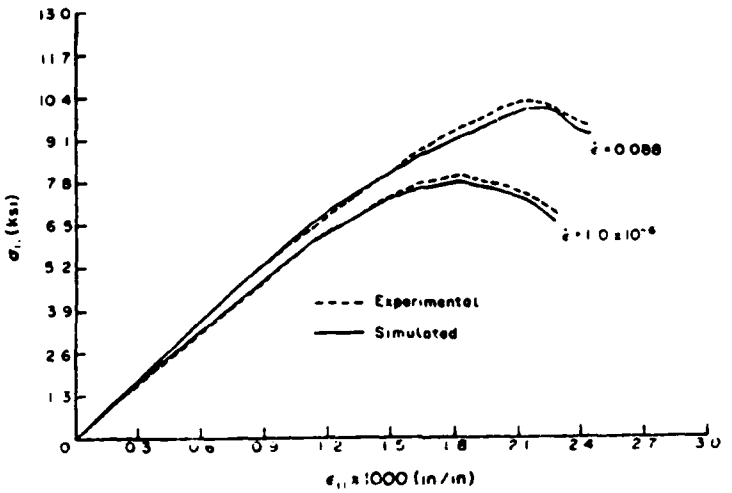

Figure 25. Comparison of the experimental and simulated dynamic stress-strain curves for uniaxial compression test of concrete specimens. The specimens are under two different constant strain rates. The elasto-viscoplastic-visco-damage model is employed in this numerical simulation.[75]

TABLE 7

SPECIFIC FEATURES OF THE SIMO AND JU MODEL
[References 76,77]

ELASTIC-VISCOPLASTIC-VISCODAMAGE MODULI

- Continuum damage using Helmholtz or Gibbs Free Energy
- Both tension and compression
- Three-dimensional stress state
- Isotropic/anisotropic

DEFINITION OF DAMAGE

- Scalar or tensor
- Elements of the moduli or their scalar multipliers are treated as internal damage variable

MICROCRACK DISTRIBUTION

- No explicit formulation

DAMAGE GROWTH LAW

- For a given local history of strain (or stress) the actual damage moduli are based on a maximum of damage dissipation
- For static loading the damage yield surface is a function in strain space or stress space
- Dynamic effects are built into the model through a viscosity parameter as usually modeled in visco-plasticity based theories for metals

FAILURE CRITERIA

- The moduli go to zero as damage reaches its critical value

modeled explicitly. Since the damage is anisotropic and mode 1 crack opening is considered, this model should be able to describe the pressure effects. The salient features of this model are:

- models crack opening (dilatancy)
- includes effects of both brittle and ductile inelastic strains
- strain rate effects are included
- damage growth equations are empirical
- considers anisotropic damage
- models splitting and faulting

The global features of most models described in this section (3.4) are summarized in Table 8.

3.5 COMPUTER CODE CALCULATIONS

The extreme complexity of developing and executing experiments on ceramic materials necessitates that the development of models for ceramic impact behavior occur through an iterative process where models are proposed, implemented, and evaluated in computational frameworks rather than developed independently. That is, models are suggested and used to permit interpretations of experiments whose interpretations may be readjusted as a result of the calculations with the trial models. Thus, computer code calculations are not only an end for the application of ceramic impact and failure models, but also a means to develop those models.

For impact of ceramics at high velocity, computational methods capable of considering stress wave propagations are necessary to adequately model the impact events. Therefore, continuum mechanics codes termed hydrocodes (but employing full stress and strain treatments of material behavior) are most often

TABLE 8

GLOBAL FEATURES OF THE REVIEWED DAMAGE MODELS FOR BRITTLE MATERIALS

AUTHORS/ YEAR	LOADING CONDITION	TENSION MODEL	COMPRESSION MODEL	STRAIN RATE EFFECT	ASSUMPTIONS	FEATURES
Curran, Seaman & Shockey [1985]	Dynamic	Micromechanics/ microstatistical	----	yes	Isotropic	Fragment statistics
Grady & Kipp [1984]	Dynamic	Continuum damage	none	yes	Isotropic	Fragmentation
Taylor, Chen, & Kuszmaul [1986]	Dynamic	Continuum damage/ fracture mechanics	Plasticity	yes	Isotropic	Fragmentation and softening
Margolin [1984]	Dynamic	Micromechanics/ fracture mechanics	Micromechanics/ fracture mechanics	yes	Isotropic damage	Faulting with confinine presure
Costin & Stone [1987]	Static	-----	Continuum damage fracture mechanics	no	Anisotropic	Softening, axial splitting and faulting
Horii & Nemat-Nasser [1983,1985]	Static	Micromechanics	Micromechanics	no	Isotropic (tension) 2-D anisotropic (compression)	Faulting and softening
Krajcinovic & Fonella [1986,1988]	Static	Micromechanics/ fracture mechanics	Micromechanics/ fracture mechanics	no	Anisotropic	Axial splitting, faulting and confinement
Ilankamban & Krajcinovic [1986,1988]	Static	Continuum damage/ phenomonological	Continuum damage/ phenomonological	no	Anisotropic,	Axial splitting, faulting
Simo & Ju [1987]	Static or dynamic	Continuum damage or plasticity/ phenomonological	Continuum damage or plasticity/ phenomonological	yes	Anisotropic	Splitting, faulting

used. Two-dimensional, explicit, finite difference or finite element codes such as EPIC-2 [Reference 78], HULL [References 79,80], HEMP [Reference 81], DYNA2D [Reference 82], and others have been used to simulate ceramic impact problems. No results have been published yet using three dimensional codes. Quasi-static failure and constitutive models most often have been developed and implemented in special purpose, implicit finite element codes.

3.5.1 Armor Penetration

Most of the reported applications of ceramic impact modeling recently have been associated with armor penetration mechanics. Recent TACOM (Tank Automative COMmand) conferences have increasingly dealt with ceramic impact and penetration. The history of analytically examining the characteristics of confined ceramic materials as protective armors has shown interest in the topic to fluctuate extensively over the past 20 to 30 years. Pioneering work by Wilkins examined the performance of light armors (such as might be applicable to personnel armors or very light vehicle armors). This work resulted in the establishment of some of the earliest dynamic measurements for ceramic impact properties, and included some of the first finite element analysis of ceramic impact events. More recent ceramic impact applications have involved confined ceramics suitable for ground mobile targets requiring heavier protection. This has meant a shift in response mechanisms in the armors from a more structural response in the light armors, to an extremely complex response of contemporary ceramic materials.

3.5.2 Simple Models

Wilkins employed the two dimensional HEMP hydrocode in a computational analysis of the impact and penetration of thin ceramic laminate armor [Reference 57]. He used the following

simplified failure criteria: (1) fracture initiates on a surface, (2) a maximum principal stress greater than 0.3 GPa in tension causes fracture, (3) there is a time delay for the complete fracture of a zone, (4) a fractured zone becomes a source for the fracture of a neighboring zone, and (5) fracture occurs only within a range of distance equal to or less than the time step times the crack velocity in ceramic.

The results of Wilkins' analysis agreed well with experimental data on thin ceramic armor penetration obtained using flash radiography.

3.5.3 Mohr-Coulomb Model

The application of a Mohr-Coulomb failure criterion to ceramics is a natural simple modeling approach for materials with such an extreme ratio of compressive to tensile strength. Most ceramics fall in a range of compressive to tensile strength ratios between 10 and 20. Although in some limited applications, it may be practical to consider tensile failures to be so predominant that a simple maximum principle tensile stress failure criterion is reasonable, for very high velocity impact problems it is easy to demonstrate that both compressive and tensile failures are significant. For two-dimensional calculations of ceramic impact, in particular, it is very simple to visualize the effects of the Mohr-Coulomb model. This approach suffers because it is an instantaneous failure criterion, providing no supporting information for the degradation of the ceramic material from one material state (solid) to another (fragmented into various sizes, with constitutive behavior dependant upon this state).

3.5.4 Griffith Model

Griffith [Reference 53] proposed a fracture criterion for glass like brittle solids, which stated that a flaw (crack) will extend in an unbounded manner when the decrease in

potential energy due to the creation of a new surface (extension of the flaw) is equal to the increase in surface energy. This criterion was originally proposed for static loading conditions. The field of fracture mechanics evolved from this criterion. Failure of a crack contained structure due to rapid crack extension is predicted by the original and modified Griffith criteria. These criteria were mostly used to characterize a single macrocrack. Grady [Reference 62] effectively used the energy balance concept of Griffith to model dynamic fragmentation in brittle rocks. Mescall and Tracy [Reference 83] recently applied Griffith criterion to model the onset of fracture in ceramic under bi-axial compressive loads. The conditions for the onset of fracture is given by:

$$\sigma_3 = \sigma_{cr} \quad \text{if } (3\sigma_3 + \sigma_1) > 0 \tag{9a}$$

$$(\sigma_3 - \sigma_1)^2 - 8\sigma_{cr}(\sigma_3 + \sigma_1) = 0 \quad \text{if } (3\sigma_3 + \sigma_1) < 0 \tag{9b}$$

where σ_1 and σ_3 are the applied compressive stresses as shown in Figure 26. σ_{cr} is the uniaxial tensile strength. The failure envelope from these equations is shown in Figure 27. In this figure, the envelopes based on the original Griffith [Reference 53] fracture criterion and the McClintock and Walsh [84] modified criterion to account for the frictional effects in closed cracks are plotted. When one of the stress components is tensile, the ceramic is assumed to fail at relatively low stress values compared to when both the stress components are compressive. This clearly is the characteristic of all ceramic materials.

Margolin [Reference 54] generalized the crack extension criterion of Griffith by considering penny shaped cracks in a spatially uniform, but otherwise arbitrary state of stress. He also included the frictional effects in closed sliding cracks under normal compressive loads. The fracture

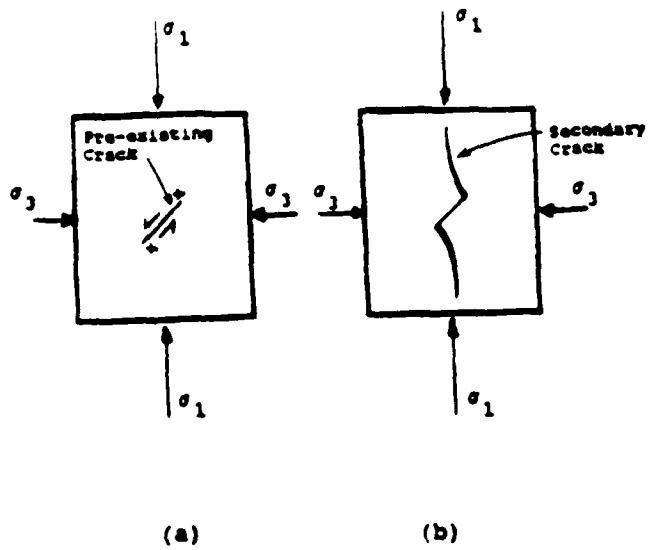

Figure 26. Triaxial compression test of brittle solid containing flaw. [80]

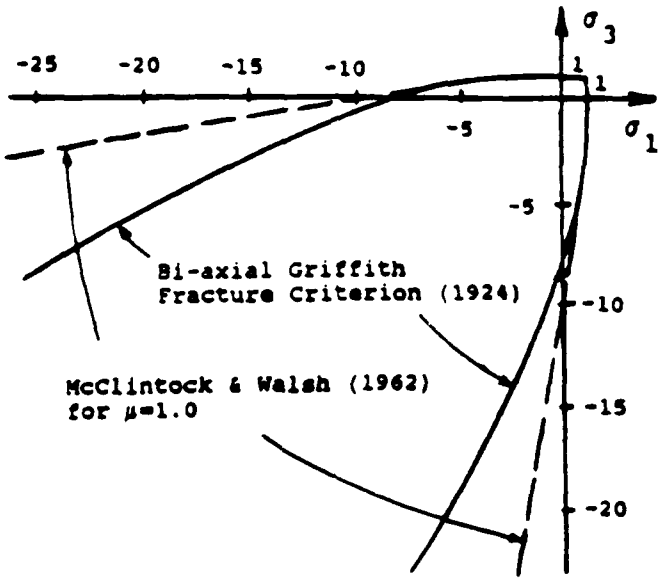

Figure 27. **Fracture locus for biaxial stress states in both tension (first quadrant) and compression (third quadrant). [80]**

criterion without frictional effects under triaxial stress and normal tension is given by:

$$\sigma_3^2 + \frac{2}{2-\nu} \quad (\sigma_{13}^2 + \sigma_{23}^2) \geq \frac{\pi TE}{2(1-\nu^2)\ C} \tag{10}$$

The stress orientations are shown in Figure 28. σ_{13} and σ_{23} are the shear stresses and σ_3 is the stress normal (out of plane) to the crack surface. ν is the Poisson's ratio, T is the surface tension, and E is the Young's modulus. When the normal stress is compressive and the cracks are closed, frictional effects modify the above criterion as follows:

$$\left[\frac{2}{2-\nu}\right] \left[\sqrt{\sigma_{13}^2 + \sigma_{23}^2} - \tau\right]^2 \geq \frac{\pi TE}{2(1-\nu^2)\ C} \tag{11a}$$

$$\text{and } \tau = \tau_o - \mu\sigma_{33} \tag{11b}$$

τ is the frictional stress across the closed crack faces. τ_o and μ are material constants. τ_o represents cohesion and μ is the dynamic frictional coefficient. The effect of friction is to reduce the effective stress in the Griffith criterion.

In summary, the Griffith criterion based fracture criteria are very useful in the modeling of brittle fracture of ceramics, especially in computer code calculations. Mescall and Tracy [Reference 83] employed this approach in modeling the long rod penetration process into a confined aluminum oxide (Al_2O_3) ceramic target. They used the HEMP code [Reference 81] to determine the spatial and temporal stress distributions in the target plate. The material is assumed to be elastic and therefore, Hooke's law based elasticity equations are sufficient to describe the material. With the details of stress fields at each material point, Mescall and Tracy [Reference 83] applied the Griffith criterion to map the fracture zones in the target as shown in Figure 29. Since the failure envelope includes both tensile and

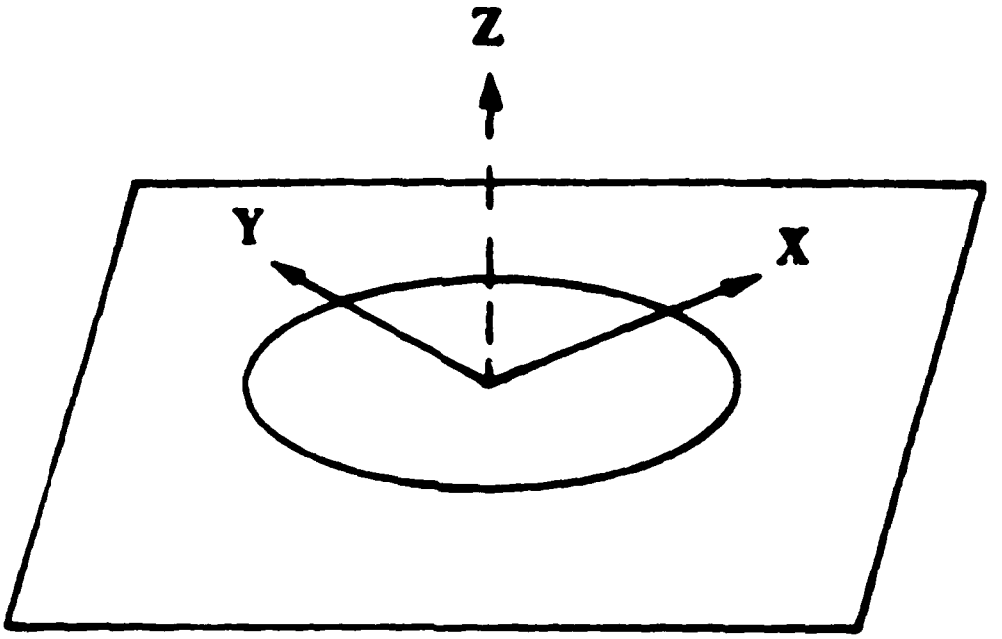

Figure 28. The crack-oriented coordinate system. [54]

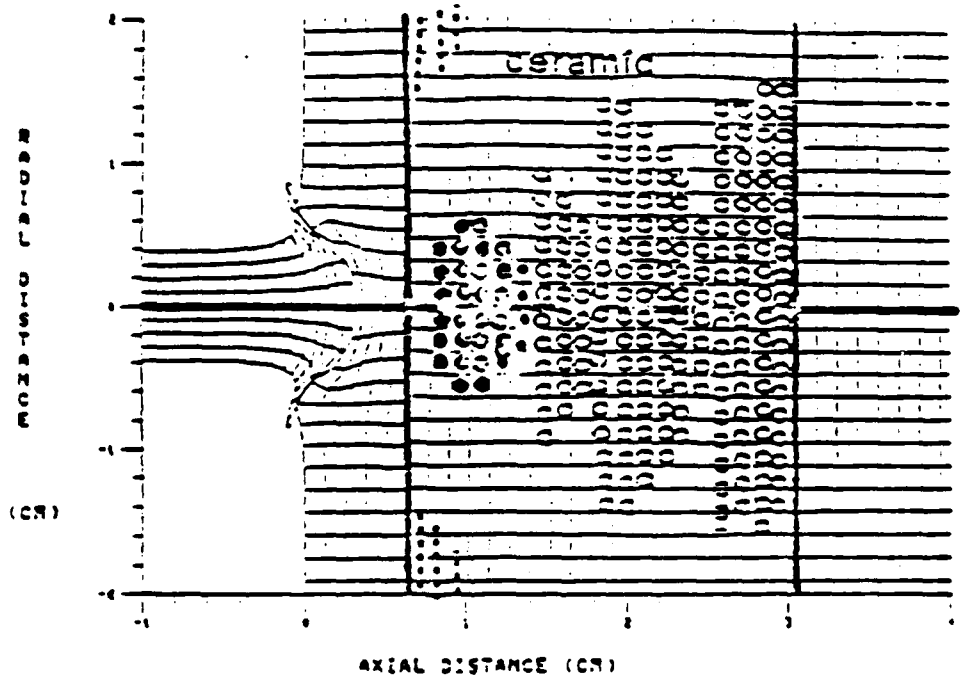

Figure 29. Fracture pattern in ceramic at five microseconds after impact. Closed circles indicate compression failure, open circles hoop tensile failure and squares radial tensile failure. [80]

compressive fractures, it is possible to show the fracture regions in terms of the failure modes. The open circles indicate fracture due to tensile hoop stress and the closed circles show the regions that fractured due to compressive stresses. The closed squares indicate fracture due to tensile radial stresses. From the computer simulations in conjunction with Griffith fracture criterion, several fracture processes were qualitatively evaluated by Mescall and Tracy [Reference 83]. Their approach provides an overall understanding of the occurrence of the fracture sequences.

In summary, it is an example application of improved, simple, instantaneous fracture criterion to describe fracture in ceramics. Most other computer simulations of the penetration processes in ceramics used simple critical stress based criterion (note that such criterion is not based on any concepts) both under tension and compression. Therefore, the use of fracture mechanics based Griffith criterion is certainly a step forward in improving fracture models for ceramics.

3.5.5 Continuum Damage Based Models

Due to the increased awareness and importance of the use of advanced constitutive and failure models for dependable results from code calculations, recently several investigators considered damage accumulation based theories to analyze ceramic response to impact loading. Margolin [Reference 42] implemented the microphysical model in a two dimensional finite difference computer code called SHALE [Reference 85] and simulated spall in a cylindrical sample of oil shale. The constitutive model that Margolin employed to describe the brittle oil shale is based on the effective elastic modulus theory for cracked bodies [Reference 68]. The effective moduli theory predicts a reduced elastic stiffness for the cracked solid. The corresponding constitutive relation takes the form:

$$\frac{d\epsilon_{ij}}{dt} = \frac{d}{dt}[C_{ijkl}\sigma_{kl}] \qquad (12)$$

where C_{ijkl} are the compliance elastic coefficients which are function of damage (crack density).

Furlong, Alme, and Rajendran [Reference 86] presented code calculations of a long rod penetration process into a confined TiB_2 ceramic target. Deformation and fracture under compression were described with plasticity based theories. Damage under compression was introduced in an ad hoc manner through a plastic work based strain rate dependent equation. The yield stress under compression was described by the Johnson-Cook model [Reference 87]. The strain rate hardening was considered, and the yield strength was relaxed by damage as follows:

$$Y = Y_o\ (1 + m\ \ln\dot{\epsilon})(1 - D) \qquad (13)$$

where Y_o is the yield strength at quasi-static loading, m is the parameter that models the strain rate dependency, and D is the scalar damage. The ceramic is assumed to lose its strength in compression completely when D reaches one. Under tension, the accumulated damage models of Kipp and Grady [Reference 65], and Taylor, Chen, and Kuszmaul [Reference 41] were employed. The damage process is described based on the fragmentation theory of Grady. Rajendran et al. [Reference 66] recently used a procedure to estimate the damage model parameters for AD85. In this procedure, the parameters are calibrated by matching the simulated and experimental stress histories in a normal plate impact test. Furlong et al. [Reference 86] used this approach and attempted to determine the damage model parameters for TiB_2 ceramic.

In the numerical modeling of ceramic penetration experiments, they compared simulation results with and without the description of damage under compression. Also, by assuming an arbitrarily low value for the Wiebull parameter "k" Furlong et

al. [Reference 83] showed the erosion of the projectile during the penetration into ceramic as shown in Figure 30. It is also found that when the value for k is increased, penetration depth into the aluminum backup plate substantially increased.

An ad hoc description of the compression fracture may be useful as an approximate engineering tool, but it will not lead to any scientific prediction tool. Model parameters can be calibrated to reproduce one of the penetration experiments without any guarantee to model another configuration of the same nature. Therefore, for predictive capabilities of computer code calculations, several key issues are yet to be resolved.

To use the computer code simulations as predictive tools for describing the penetration process into ceramics, the following issues require attention:

1. Description of fracture under combined compressive and shear loading.
2. Strain rate and temperature effects on the strength of intact ceramic.
3. Determination of damage evolutions under shock loading.
4. Properties of the pulverized ceramic with and without confining pressures.
5. Accurate descriptions for the equation of state.
6. Behavior of ceramic under unloading and reloading.
7. Effects of previous loading history on strength and fracture process.
8. Directional dependency of damage evolution (damage induced anisotropy).

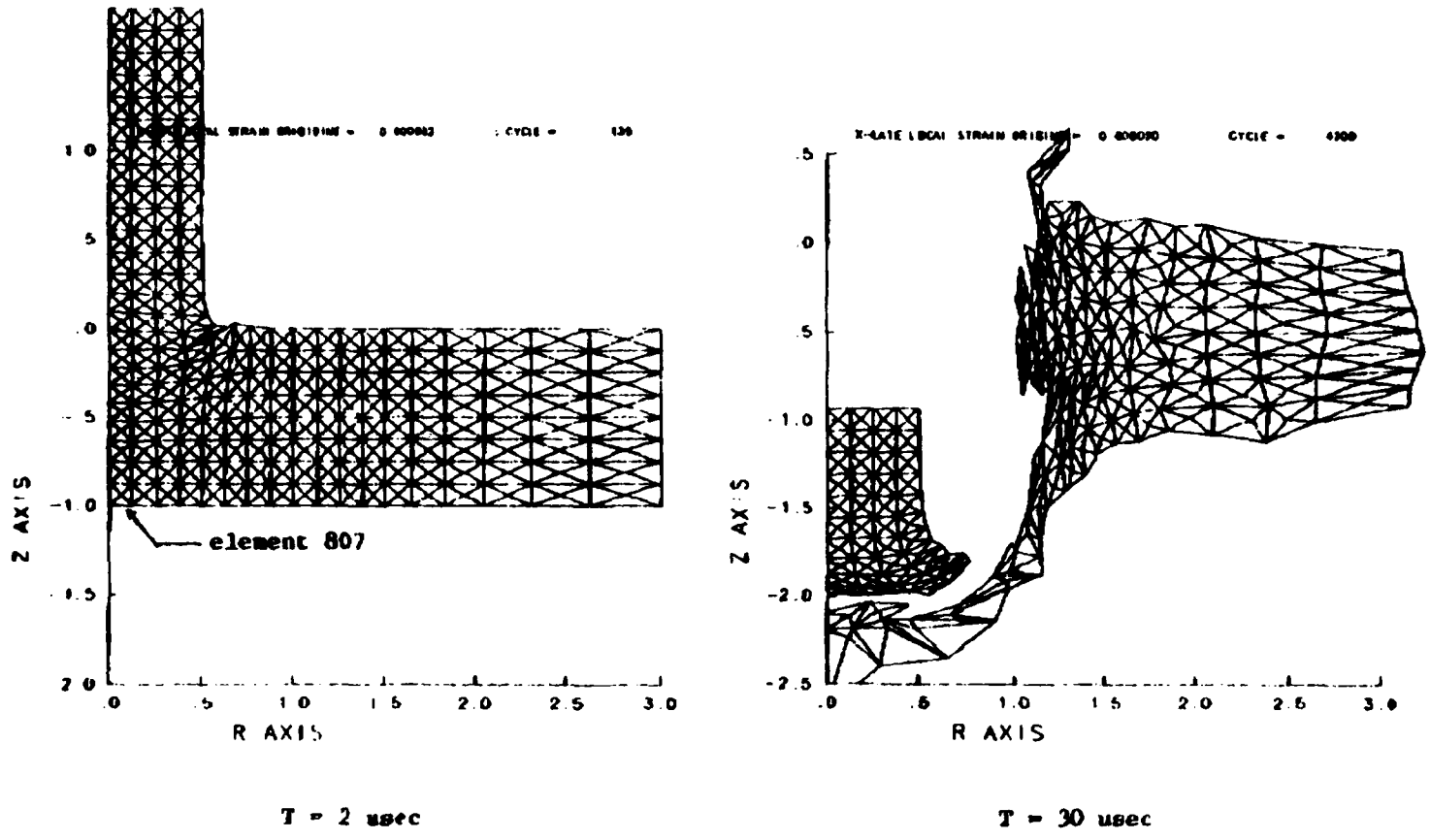

Figure 30. Long rod penetration into a ceramic target. [83]

SECTION 4
SUMMARY AND CONCLUSIONS

Based on the review of the dynamic experimental techniques, it appears that most investigations for evaluating ceramic material response under impact loading employed flyer plate impact (which include double flyer plate and recovery tests), long rod impact, and Hopkinson bar tests. Some penetration experiments are also reported. Among the most significant results, the strain rate and confining pressure effects on the compressive strength and the sensitivity of the spall (tensile) strength of ceramics to the HEL value seem to be the most important results. Experimental evidence exists that at shock velocities at and above the HEL, the tensile strength of ceramics such as Al_2O_3 alumina and sodalime glass is reduced to zero. Below the HEL, sodalime sustained a tensile strength comparable to the theoretical limit of the material. Similarly the shear strength of single crystals such as quartz and MgO is found to decrease significantly above the HEL. Unlike single crystals, polycrystalline ceramics in most cases did not lose their shear strength especially aluminum oxide without any alloying elements (99.9% pure Al_2O_3). Conflicting results are also observed regarding the precursor decay phenomenon. While Yaziv et al. [Reference 20] found a strong precursor decay in commercial AD-85 alumina, Cagnoux and Longly [Reference 21] showed that 95% Al_2O_3 commercial alumina did not exhibit any precursor decay. In a recent conference proceeding [Reference 88], several articles appear focussing on these results. These results indicate that the effects of strain rate on the compressive strength is yet to be fully evaluated. Results from penetration experiments showed that there is a threshold penetrator velocity above which a confined plate is more effective in resisting penetration as compared to a metal plate [Reference 36].

Since response of ceramics unlike concrete and rock under static loading conditions is generally elastic and Hooke's law based constitutive modeling of the stress-strain response is adequate. However under dynamic loading, ceramics are found to exhibit significant amount of inelastic deformation as well as strong strain rate and confining pressure dependence. Therefore, a higher degree of sophistication is required to realistically model the dynamic response. Aside from the empirical models which are developed based on curve fitting of experimental data and used to describe specific phenomena, we are able to identify five distinct modeling approaches. In the first approach, elastic behavior is assumed and Hooke's law is used to calculate the stresses. Failure is then predicted using Griffith's fracture criterion. In the second approach, elastic-plastic behavior is assumed. A yield surface (which may be pressure dependent) separates elastic and plastic regimes, and the calculations of inelastic stresses are performed using the equations developed for metal plasticity. The details of crack growth are ignored and the strain rate effect may be included by modifying the flow rule. In the third approach, fracture mechanics based microphysical theories are employed to describe the compressive failure processes. In this approach, elasticity equations based on Hooke's law are combined with effective moduli (reflecting material damage) to model the material response. Material failure is predicted based on a critical evolution of the microstructure. In the fourth approach, microstatistical based fracture models are considered. In this type of modeling, most of the emphasis is placed on statistical distribution of the microstructure (cracks, voids, etc.) and the formulation is not necessarily within the framework of fracture mechanics and micromechanics theories. In the last approach, several continuum damage mechanics based models are considered.

In summary, most of these approaches are derived and employed for describing brittle materials such as the concrete, rocks, oil shale, etc., under both quasi-static and impact loading. The present review clearly indicates that a combined analytical, numerical and experimental studies are required to fully understand and model the complex impact behavior of ceramic materials. The thrust of these studies should be to evaluate and model the effects of material variables on the ultra-high strain rate response of brittle materials leading to the formulation of appropriate constitutive models. These models should be based on the observed deformation and fracture mechanisms at both the micro and macro scales. The ability to accurately predict dynamic, inelastic structural response, such as projectile penetration into ceramic targets, depends on the development of such constitutive and failure models.

REFERENCES

1. Ahrens, T.H., Gust, W.H., and Royce, E.B., J. Appl. Phys. 39, (1968), p 4610.

2. Gust, W.H. and Royce, E.B., J. Appl. Phys., 42, (1971), p 274.

3. Gust, W.H., Holt, A.C., and Royce, E.B., "Dynamic Yield, Compressional, and Elastic Parameters for Several Lightweight Intermetallic Compounds," J. Appl. Phys., Vol. 44, No. 2, (1973), p 550

4. Munson, D.E. and Lawrence, R.J. "Dynamic Deformation of Polycrystalline Alumina," J. Appl. Phys. 50, No. 10, (1979), p 6272.

5. Wilkins, M.L., in BORON AND FRACTORY BORIDES, edited by V.I. Matkovis, The Carborundum Comp., (1977), pp. 633-648.

6. McQueen, R.G., Marsh, S.P., Taylor, J.W., Frintz, J.N., Carter, W.J., in HIGH VELOCITY IMPACT PHENOMENA, edited by R. Kinslow, Academic Press, (1970), pp. 294-415.

7. Dremin, A.N., Adadurov, G.A., Sov. Phys. Solid St. 6, 1379 (1964).

8. Rosenberg, Z., Yeshurun, Y., Brandon, D.G., "Dynamic Response and Microstructure of Commercial Alumina," J. Phys. (Paris) Colloq. 5, (1985), pp. C5-331.

9. Graham, R.A. and Brooks, W.P., J. Phys. Chem. Solids 32, (1971), p 2311.

10. Barker, L.M. and Hollenback, R.E., "Shock Wave Studies of PMMA, Fused Silica, and Sapphire," J. Appl. Phys., Vol. 41, No. 10, (1970), p 4208.

11. Wackerle, J., J. Appl. Phys., 33, (1962), p 922.

12. Fowles, G.R., J. Geophys. Res., Vol. 72, (1967), p 5729.

13. Ahrens, T.J., J. Appl. Phys. 37, (1966), p 2530.

14. Grady, D.E., in 'High Pressure Research, Applications in Geophysics,' edited by M.H. Manghnani, S. Akimoto, Acad. Press, (1977), pp. 389-438.

15. Ahrens, T.J. and Linde, R.K., in 'Behavior of Dense Media under High Dynamic Pressure,' ed. by J. Beyer, Gordon-Breach (1968), pp. 316-336.

16. Rosenberg, Z., Yaziv, D., Yeshurun, Y., and Bless, S.J., "Shear Strength of Shock Loaded Alumina as Determined with Longitudinal and Transverse Manganin Gauges," J. Appl. Phys., Vol. 62, No. 3, (1987), pp. 1120-1122.

17. Bless, S.J. and Ahrens, T. J., J. Geophys. Res. 81, (1976), p 1935.

18. Rosenberg, Z., Yaziv, D., and Bless, S.J., "Spall Strength of Shock Loaded Glass," J. Appl. Phys., Vol. 58, No. 8, (1985), pp. 3249-3251.

19. Asay, J.R., Fowles, G.R., Durall, G.E., Miles, M.H., and Tinder, R.F., J. Appl. Phys. 43, (1972), p 2132.

20. Yaziv, D., Yeshurun, Y., Partom, Y., and Rosenberg, Z., "Shock Structure and Precursor Decay in Commercial Alumina," in 'Shock Waves in Condensed Matters,' ed. by S.C. Schmidt and N.C. Holmes, Elsevier Sciencs Pub., (1987), p 359.

21. Cagnoux, J., and Langy, F., "Is the Dynamic Strength of Alumina Rate Dependent?" in 'Shock Waves in Condensed Matters,' ed. by S.C. Schmidt and N.C. Holmes, Elsevier Sciences Pub, (1987).

22. Yaziv, D., "Shock Fracture and Recompaction of Ceramics," Ph.D. Thesis, University of Dayton, July 1985.

23. Majewski, P., Gupta, Y.M., and Seaman, L., "Tension-Recompression Response of Shock Loaded Polycarbonate," in 'Shock Waves in Condensed Matters,' ed. Y.M. Gupta, Plenum Press, NY, 1986.

24. Nicholas, T., "Tensile Testing of Materials at High Rates of Strain," Exp. Mech., 21, (1981), pp. 177-185.

25. Lindholm, U.S., "Some Experiments with the Split Hopkinson Pressure Bar," J. Mech Phys. Solids, 12, (1964), pp. 317-335.

26. Malvern, L.E., Tang, R., Jenkins, D.A., and Gong, J.C., "Dynamic Compressive Strength of Cementitious Materials," Mat. Res. Soc. Symposia Proceedings Cement Based Composites: Strain Rate Effects on Fracture, ed. by S. Mindess and S.P. Shah, Vol. 64, (1986), pp. 119-138.

27. Jawed, I., Childs, G., Ritter, A., Winzer, S., Johnson, T., and Barker, D., "High Strain Rate Compressive Behavior of Hydrated Cement Pastes," Cement and Concrete Research, Vol. 17, (1987), pp. 433-440.

28. Lankford, J., Soc. Petrol. Eng. Jour., Vol. 17, (1976), p 17.

29. Lankford, J., "The Role of Tensile Microfracture in the Strain Rate Dependence of Compressive Strength of Fine-Grained Limestone - Analog with Strong Ceramics," Int. J. Rock Mech. Min. Sci. and Geomech. Abstra., Vol. 18, (1981), pp 173-175.

30. Rosenberg, Z., Mayseless, M., and Partom, Y., "The Use of Manganin Stress Transducers in Impulsively Loaded Long Rod Experiments," J. Appl. Mech, Vol. 51 (1984).

31. Rosenberg, Z. and Bless, S.J., "Determination of Dynamic Yield Strengths with Embedded Manganin Gauges in Plate-Impact and Long-Rod Experiments," Exp. Mech., Vol. 26, (1986), pp. 279-282.

32. Kuscher, G., Hohler, B., and Stilp, A.J., "Non-Linear Propagation of Elasto-Plastic Waves in Rods," 4th APS Topical Conf. on Shock Waves in Condensed Matter, (July 1985), pp. 377-382.

33. Brar, N.S., Bless, S.J., and Rosenberg, Z, "Brittle Failure of Ceramic Rods Under Dynamic Compression," to be published in 2nd International Conference of Mechanical and Physical Behavior of Materials under Dynamic Loading, Ajaccio, France, September 1988.

34. Wilkins, M.L., Cline, C.F., and Honodel, C.A., Lawrence Radiation Laboratory Report UCLR-50694, 1969.

35. Wilkins, M.L., Landingham, R.L., and Honodel, C.A., Lawrence Radiation Laboratory Report UCLR-50980, 1971.

36. Mayseless, M., Goldsmith, W., Virostek, S.P., and Finnegan, S.A., "Impact on Ceramic Targets," ASME, J. Appl. Mech., Vol. 54, (1987), p 373.

37. Kennedy, J.M. and Cook. N., "Crack Models for the Failure of Rocks in Compression," in Constitutive Laws for Engineering Materials Theory and Applications, ed. by C.S. Desai, E.K. Krempl, P.D. Kiousis, and T. Kundu, Elsevier Sciences Pub., (1987), p 879.

38. Shockey, D.A., Curran, D.R., Seaman, L., Rosenberg, J.T., and Petersen, C.F., "Fragmentation of Rock under Dynamic Loads," Int. J. Rock. Mech. Sci. and Geomech. Abstr., Vol. II, (1974), pp. 303-317.

39. Grady, D.E. and Kipp, M. E., "Continuum Modeling of Explosive Fracture in Oil Shale," Int. J. Rock Mech. Min. Sci. and Geomech. Abstr., Vol 17, (1980), pp. 147-157.

40. Costin, L.S. and Holcomb, D.J., "A Continuum Model of Inelastically Deformed Brittle Rock Based on the Mechanics of Microcracks," in Proceedings of the International Conference on Constitutive Laws for Engineering Materials, ed. by C.S. Desi, and R.H. Gallagher, (1983), pp. 185-195.

41. Taylor, L.N., Chen, E.P., and Kuszmaul, J.S., "Microcrack-Induced Damage Accumulation in Brittle Rock under Dynamic Loading," Computer Methods in Applied Mechanics and Engineering, Vol. 55, (1986), p 301-320.

42. Margolin, L.G., "Numerical Simulation of Fracture," in Proceedings of International Conference on Constitutive Laws for Engineering Materials, eds. C.S. Desai and R.H. Gallagher, Tucson, AR, (Jan. 1983), pp. 567-572.

43. Brandt, R.C., Hasselman, D.P.H., and Lange, F.F., "Fracture Mechanics of Ceramics", Plenum Press, NY, 1983.

44. Rice, R.W., Freiman, S.W., Pohanka, R.C., Mecholesky, J.J., Jr., and Wu, C.C., "Microstructural Dependence of Fracture Mechanics Parameters in Ceramics," Fracture Mechanics of Ceramics, Vol. 4, eds., R. C. Bradt, et al., Plenum Press, NY, (1978), pp. 848-876.

45. Marsh, D.M., "Flow and Fracture in Glass," Fracture of Solids, ed. by D.C. Drucker and J.J. Gilman, Wiley & sons, New York, (1963), pp. 143-155.

46. Lawn, B.R., "Physics of Fracture," J. Am. Ceramic Soc., Vol. 66, (1983), pp. 83-91.

47. Hockey, B.J., "Crack Healing in Brittle Materials," in Fracture Mechanics of Ceramics, Vol. 6, ed. by R.C. Bradt, D.P.H. Hasselman, and F.F. Lange, Plenum Press, New York, (1983), pp. 637-658.

48. Ohr, S.M. and Kobayashi, S., "In-Situ Observation of Crack Propagation by Transmission Electron Microscopy," J. of Metals, Vol. 32(5), (1980, p 35.

49. Chen, A.C. and Chen, W.F., "Constitutive Relations for Concrete," J. Eng. Mech. Div., ASCE, Vol. 101 (EM4), (1985), p 465.

50. Takahashi, Y., "Elastic-Plastic Constitutive Modeling of Concrete," Argonne National Laboratory Report, ANL-83-23, 1983.

51. Dragon, A. and Mroz, Z., "A Continuum Model for Plastic-Brittle Behavior of Rock and Concrete," Int. J. Engg. Sci., Vol. 17, (1979), pp. 121-137.

52. Bazant, Z.P. and Kim, S., "Plastic-Fracturing Theory for Concrete," J. Eng. Mech. Div, ASCE, Vol. 105 (EM3), (1979), pp. 407-428.

53. Griffith, A.A., "The Phenomena of Rupture and Flow in Solids," Phil. Trans. of Royal Soc. of London, Vol. 221, (1920), pp. 163-198.

54. Margolin, L.G., "A Generalized Griffith Criterion for Crack Propagation," Engineering Fracture Mechanics, Vol. 19(3), (1984), pp. 539-543.

55. Wilkins, M.L., "Calculation of Elastic-Plastic Flow," Lawrence Livermore Laboratory, UCRL-7322, Rev. 1, 1969.

56. Glenn, L.A., CERAC Report No. 22, 1974.

57. Wilkins, M.L., "Mechanics of Penetration and Perforation," Int. J. Eng. Sci., Vol. 16, (1978), pp. 793-807.

58. Glenn, L.A., "The Fracture of a Glass Half-Space by Projectile Impact," J. Mech. Phys. Solids, Vol. 24, (1976), pp. 93-106.

59. Curran, D.R., Seaman, L., and Shockey, D.A., "Dynamic Failure of Solids," Physics Report, Vol. 147, pp. 253-388 (1987).

60. Curran, D.R., Seaman, L., and Shockey, D.A., "Linking Dynamic Fracture to Microstructural Processes," in Shock Waves and High Strain Rate Phenomena in Metals, ed. M.A. Meyers and L.E. Murr, Plenum Press, N.Y., pp. 129-167 (1981).

61. Curran, D.R., Shockey, D.A., and Seaman, L., "Dynamic Failure in Solids," J. Appl. Phys., Vol. 44, (1973), p 4025.

62. Grady, D.E., "Local Inertia Effects in Dynamic Fragmentation," J. Appl. Phys., Vol 53, (1982), pp. 322-325.

63. Glenn, L.A. and Chudnovsky, A., "Strain Energy Effects on Dynamic Fragmentation," J. Appl. Phys., Vol. 59, No. 4, (1986), pp. 1379-1380.

64. Glenn, L.A., Gommerstadt, B.Y., and Chudnovsky, A., "A Fracture Mechanics Model of Fragmentation," J. Appl. Phys., Vol. 60, No. 3, (1986), pp. 1224-1226.

65. Kipp, M.E. and Grady, D.E., "Dynamic Fracture Growth and Interaction in One Dimension," J. Mech. Phys. Solids, Vol. 33, (1985), pp. 399-415.

66. Rajendran, A.M., Kroupa, J., and Brar, N.S., "Modeling of Ceramic Material Under Impact Loading," UDR-TM-87-32, University of Dayton Research Institute, Dayton, OH, September 1987.

67. Margolin, L.G., "Microphysical Models for Inelastic Material Response," International Journal of Engineering Science, Vol. 22, No. 8-10, (1984), pp. 1171-1179.

68. Margolin, L.G., "Elastic Moduli of a Cracked Body," International Journal of Fracture, 22, (1983), pp. 65-79.

69. Costin, L.S. and Stone, C.M., "Implementation of a Finite Element Damage Model for Rock," Constitutive Laws for Engineering Materials, Theory and Applications, II, eds. C.S. Desi, et al., Elsevier Science Publishing Co., Inc., (1987), pp. 829-841.

70. Costin, L.S. and Stone, C.M., "A Finite Element Material Model for Microfracture - Damaged Brittle Rock," Sandia Report, SAND87-1227, UC-13, 1987.

71. Horii, H. and Nemat-Nasser, S., "Compression-Induced Microcrack Growth in Brittle Solids: Axial Splitting and Shear Failure," Journal of Geophysical Research, Vol. 40, No. B4, (1985).

72. Horii, H. and Nemat-Nasser, S., "Overall Moduli of Solids with Microcracks: Load-Induced Anisotropy," Journal of Mechanical Physics of Solids, Vol. 31, No.2, (1983).

73. Horii, H. and Nemat-Nasser, S., "Brittle Failure in Compression: Splitting, Faulting, and Brittle-Ductile Transition," Phil. Trans. R. Soi, London, Vol. 319, (1986), pp. 337-374.

74. Krajcinovic, D. and Fanella, D., "A Micromechanical Model for Concrete," Engg. Fracture Mech., Vol. 25, Nos. 5/6, (1986), pp. 585-596.

75. Ilankamban, R. and Krajcinovic, D., "A Constitutive Theory for Progressively Deteriorating Brittle Solids," Int. J. Solids Structures, Vol 23(11), (1987), pp. 1521-1534.

76. Simo, J.C. and Ju, J.W., "Strain- and Stress-Based Continuum Damage Models - I Formulation," Int. J. Solids Structures, Vol. 23, No. 7, (1987), pp. 821-840.

77. Simo, J.C. and Ju, J.W., "Strain- and Stress-Based Continuum Damage Models - II Computational Aspects," Int. J. Solids Structures, Vol. 23, No. 7, (1987), pp. 841-869.

78. Johnson, G.R. and Stryk, R.A., "User Instructions for the EPIC-2 Code," AFATL-TR-86-51, August 1986.

79. Gaby, L.P., "HULL System Guide," Air Force Weapons Laboratory Report C4-C-4041, 1978.

80. Durrett, R.E. and Matuska, D.A., "The HULL Code - Finite Difference Solution to the Equations of Continuum Mechanics," Air Force Armament Laboratory, AFATL-TR-78-125, 1978.

81. Giroux, E.D., "HEMP User's Manual," Lawrence Livermore Laboratory, UCRL-51079, Rev. 1, 1973.

82. Hallquist, J.O., "DYNA2D - An Explicit Finite Element and Finite Difference Code for Axisymmetric and Plane Strain Calculations (User's Guide)," Lawrence Livermore Laboratory, UCRL-52429, 1978.

83. Mescall, J.F. and Tracy, C.A., "Improved Modeling of Fracture in Ceramic Armors," presented at Army Science Conference, June 17-19, 1986.

84. McClintock, F.A. and Walsh, J.B., "Friction on Griffith Cracks," Proc. of the 4th U.S. Nat. Cong. Appl. Mech., Berkely, CA, (1962), pp. 1015-1021.

85. Amsden, A.A., Ruppel, H.M., and Hirt, C.W., "SALE: A Simplified ALE Computer Program for Fluid Flow at All Speeds," Los Alamos National Laboratory Report LA-8095, 1980.

86. Furlong, J., Alme, M., and Rajendran, A.M., "Numerical Modeling of Ceramic Penetration Experiments," Proceedings of TACOM Armor Coordinating Conference for Light Combat Vehicles, (1988).

87. Johnson, G.R. and Cook, W.H., "A Constitutive Model and Data for Metals Subjected to Large High Strain Rates and High Temperatures Pressures," Proc. 7th Int. Symp. on Ballistics, The Hague, The Netherlands, April 1983, pp. 541-547.

88. Proceedings of 2nd International Conference on Mechanical and Physical Behavior of Materials under Dynamic Loading held at Ajaccio, France, September 19-23, 1988.